2017-01-01

# Development And Integration Of The Janus Robotic Lander: A Liquid Oxygen - Liquid Methane Propulsion System Testbed

Raul Ponce
*University of Texas at El Paso*, ponce_raul@ymail.com

DEVELOPMENT AND INTEGRATION OF THE JANUS ROBOTIC LANDER:
A LIQUID OXYGEN-LIQUID METHANE
PROPULSION SYSTEM TESTBED.

RAUL PONCE

Master's Program in Mechanical Engineering

APPROVED:

Ahsan Choudhuri, Ph.D., Chair

John F. Chessa, Ph.D., Co-Chair

Luis R. Contreras-Sapien, Ph.D.

Charles Ambler, Ph.D.
Dean of the Graduate School

## Dedication

To:

My mother Griselda,
for she has always guided me through life never lacking love, encouragement and prayer.
Always pushing me to become a better man.

My father Raul,
for always giving me his advice and support. His work as an engineer inspired me to become an engineer myself.

My sister Gris,
who has given me a wonderful goddaughter and soon a baby nephew. I strive to always be a positive role model for them as she has been for me.

My girlfriend Caro,
who always gives me inspiration and encouragement and on whom I can always rely to put a smile on my face.

My grandmother, Mache, and my godparents Alma and Chu,
thank you for being there in all the good and bad moments.

The rest of my friends and family.

# DEVELOPMENT AND INTEGRATION OF THE JANUS ROBOTIC LANDER: A LIQUID OXYGEN-LIQUID METHANE PROPULSION SYSTEM TESTBED

by

RAUL PONCE, B.S. Mechanical Engineering

THESIS

Presented to the Faculty of the Graduate School of

The University of Texas at El Paso

in Partial Fulfillment

of the Requirements

for the Degree of

MASTER OF SCIENCE

Department of Mechanical Engineering

THE UNIVERSITY OF TEXAS AT EL PASO

May 2017

## Acknowledgements

First of all, I would like to thank my advisor and committee chair Dr. Ahsan Choudhuri for the opportunity of doing research at the cSETR. Thanks to this opportunity I was introduced to the field of aerospace which I enjoy so much and has opened doors to work in amazing projects with NASA and now Lockheed Martin. I would also like to thank the rest of my committee, Dr. Chessa and Dr. Contreras for taking the time to review my work.

Thank you also to my mentors Mr. Scott Hill and Dr. Jack Chessa for always providing their guidance and sharing their expertise in this project and in engineering in general. I would also like to thank Mr. J.C. Melcher from JSC and Mr. Eduardo Seyffert from Blue Origin for taking the time to give us their technical guidance. Their constant advice was always extremely helpful.

Special recognition and thanks goes to all the students who have contributed to this project either directly or indirectly. Luz Bugarin, Israel Lopez, Pedro Nuñez, Linda Hernandez, Mariana Chaidez, Abner Moreno, Jason Adams, Marissa Garcia, Jahir Fernandez, Aaron Johnson, Dylan Ott, Steven Torres, Jo Carroll, David Lemon, thank you for your diligence and hard work. I had a lot of fun solving problems together.

Lastly, thank you to the Mechanical Engineering Department and all the cSETR staff as well as the rest of the students in Casita. Thanks to you my time spent as a graduate student went smoothly and was really enjoyable.

# Abstract

Initiatives have emerged with the goal of sending humans to other places in our solar system. New technologies are being developed that will allow for more efficient space systems to transport future astronauts. One of those technologies is the implementation of propulsion systems that use liquid oxygen and liquid methane ($LO_2$-$LCH_4$) as propellants.

The benefits of a $LO_2$-$LCH_4$ propulsion system are plenty. One of the main advantages is the possibility of manufacturing the propellants at the destination body. A space vehicle which relies solely on liquid oxygen and liquid methane for its main propulsion and reaction control engines is necessary to exploit this advantage.

At the University of Texas at El Paso (UTEP) MIRO Center for Space Exploration Technology Research (cSETR) such a vehicle is being developed. Janus is a robotic lander vehicle with the capability of vertical take-off and landing (VTOL) which integrates several $LO_2$-$LCH_4$ systems that are being devised in-house. The vehicle will serve as a testbed for the parallel operation of these propulsion systems while being fed from common propellant tanks.

The following work describes the efforts done at the cSETR to develop the first prototype of the vehicle as well as the plan to move forward in the design of the subsequent prototypes that will lead to a flight vehicle. In order to ensure an eventual smooth integration of the different subsystems that will form part of Janus, requirements were defined for each individual subsystem as well as the vehicle as a whole. Preliminary testing procedures and layouts have also been developed and will be discussed to detail in this text. Furthermore, the current endeavors in the design of each subsystem and the way that they interact with one another within the lander will be explained.

# Table of Contents

## List of Tables

# List of Figures

# Chapter 1: Introduction and Background

## 1.1 INTRODUCTION

At the National Aeronautics and Space Administration (NASA) as well as some private spaceflight companies, a renewed interest has arisen for human space exploration. Mars is one of the destinations that has gotten more attention and resources have been assigned towards the development of technologies that will enable humans to land on the surface of Mars and return to Earth safely.

To take astronauts on such a journey, many questions need to be answered. One such question is: Which propellant should be used for an interplanetary propulsion system? One of the strongest candidates is a liquid oxygen and liquid methane propellant combination given the potential to be generated on the surface of Mars and other planets. However, $LO_2$-$LCH_4$ is a propellant combination that has never been used for space flight vehicles as of now; therefore, research needs to be done in order to make its use possible for a man-rated spacecraft.

At the MIRO Center for Space Exploration Technology Research (cSETR) of the University of Texas at El Paso (UTEP), $LO_2$-$LCH_4$-enabling technologies have been investigated for the past recent years. These include a $LO_2$-$LCH_4$ torch igniter, a 5-8 lbf reaction control engine (RCE) as well as both a 500 lbf and a 2,000 lbf $LO_2$-$LCH_4$ rocket engine. The ultimate test for these technologies will be when they are implemented onto two vehicles that are also being currently developed at the cSETR: Janus and Daedalus. A preliminary rendering of these vehicles can be seen in Figure 1. Janus is a robotic lander that will have the capability for autonomous vertical take-off and landing (VTOL) whereas Daedalus will serve as a technology demonstrator while on a suborbital flight. Both vehicles will incorporate the same RCE and torch igniter; however, Janus will employ the 2,000 lbf engine while Daedalus uses the 500 lbf engine as their main propulsion source.

**Figure 1: 3-D Rendering of Janus (left) and Daedalus (right).**

The goal of both Janus and Daedalus is to test the possibility of having a fully integrated vehicle whose propulsion needs are met with the use of only liquid oxygen and liquid methane. Providing a spacecraft with this capability reduces the complexity of the system by minimizing the number of different fluids required for its operation as well as reducing its total dry mass given the need for less tanks, tubing, etc.

This thesis will narrate the development of the Janus robotic lander in particular. Since the beginning of the program in September of 2015, the focus of the efforts done at the cSETR towards Janus have been mainly in requirements development and integration planning as well as the design of a first prototype.  In parallel, the design of its subcomponents has been done individually while requirements for their integration to the lander have also been defined.

Janus will be tested in UTEP's Technology Research and Innovation Acceleration Park (tRIAc) in Fabens, Texas 33 miles from UTEP's main campus. The layouts and procedures that have been implemented for the test of the first prototypes at the tRIAc Alpha site will also be discussed in this work.

## 1.2 Background

### 1.2.1 Using Liquid Methane ($LCH_4$) as a Propellant

One of the most critical aspects of space system design is the selection of the propellant that will be used to provide propulsion. Many different types of liquid propellants have been used for different applications: from high energy cryogenics to hypergolic and monopropellants. For the case of a relatively light-weight lander such as is Janus, almost any propellant combination would suffice to provide enough thrust for a main engine as well as a reaction control system (RCS). However, there are other aspects to consider when the end goal is a complete architecture that will allow for human exploration of another celestial body.

#### *1.2.1.1 In-Situ Resource Utilization (ISRU)*

During an interplanetary exploration mission, it would be greatly beneficial to have the capability to acquire the required propellant at the site that is being explored. Having that capability is referred to as in-situ resource utilization (ISRU).

A full system model studying the feasibility of having ISRU on the surface of Mars has been done by NASA [1]. The model was done assuming a propulsion system for a Mars Ascent Vehicle that utilizes liquid oxygen and liquid methane as propellants. It was found that a configuration such as this would reduce the required landed propellant mass by as much as 95% [1].

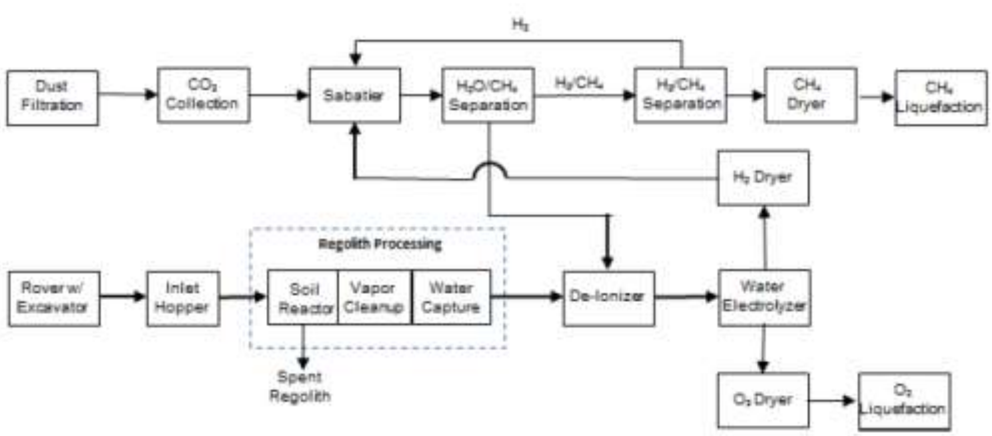


**Figure 2: Schematic of a full oxygen &methane ISRU system [1].**

$LO_2$-$LCH_4$ is not the only propellant combination with the possibility of being acquired via ISRU; however, $LO_2$-$LCH_4$ allows for a closed-loop ISRU system which would in fact produce excess oxygen to be used for crew life-support.

The methane and oxygen propellants would be produced on the surface of Mars by the use of two well-known chemical reactions: Water Electrolysis and the Sabatier Reaction. It has been discovered that there is an abundance of water on Mars; therefore, together with the profusion of carbon dioxide from Mars' atmosphere, the raw material becomes available.

As seen in the schematic of Figure 2, water would be collected from the regolith of Mars which would then be electrolyzed producing Hydrogen and Oxygen. The Oxygen could be liquified to use as a propellant or it could be used for life support; on the other hand, the resultant Hydrogen would undergo a Sabatier reaction by being combined with the carbon dioxide ($CO_2$) that was collected from the atmosphere. Water and methane would be the products of this reaction of which the water could be electrolyzed while the methane would be liquified to use as a propellant. The power needed to generate the required reactions could either be produced by a fission reactor or by solar panels.

#### *1.2.1.2 Storability*

For high-thrust applications, liquid propellants with the addition of solid boosters have become the norm in rocket engine development. Liquid propellants are a very attractive option for lower stage rocket engines due to their high-energy output. However, a difficulty lies in that most liquid propellants with a high-energy output are cryogenics. Cryogenic propellants are fluids that if allowed to reach Earth's ambient conditions would become gasses. Therefore, in order to maintain cryogenic propellants in their liquid state they must be kept at extremely low temperatures.

Ever since the Apollo era, a combination of $LO_2$ and either a refined kerosene propellant called Rocket Propellant 1 (RP-1) or liquid hydrogen ($LH_2$) have been the propellant of choice for

launch systems that require a high thrust output. These propellants have proven to be a reliable option although they have some downsides.

$LO_2$-$LH_2$ is a highly efficient propellant combination yielding a theoretical specific impulse ($I_{sp}$) of 455 s. (vacuum expansion, $P_c$=1,000 psia) [2]. It has been used successfully by numerous rocket engines such as the Space Shuttle Main Engine (SSME) and Saturn V's J-2 engine. Although it can also be acquired via ISRU, $LH_2$ has an extremely low boiling temperature of -423°F (at sea level pressure 14.7 psia) which makes it very difficult to be stored for long durations of time. Also, $LH_2$ has a very low density compared to other propellants and therefore requires a relatively large tank making a vehicle quite cumbersome. $LO_2$-$LH_2$ is therefore not suitable for deep space applications.

RP-1 on the other hand, has a much higher density than $LH_2$ making it a better choice when there are volume constraints such as was the case of the Saturn V's first stage. $LO_2$-RP-1 is a propellant combination that, although it has a lower $I_{sp}$ of 358 s. (vacuum expansion, $P_c$=1,000 psia) [2], it still provides a very high thrust output. It was used during the Apollo era by the F-1 rocket engine and it's still in use today by SpaceX on the Merlin rocket engine among others. RP-1 also has the benefit of being easily storable since it's not a cryogenic fluid. Therefore, RP-1 can be stored for longer durations without issue and removes the complexity of having a cryogenic bipropellant system. However, there is no easy way of manufacturing RP-1 on the surface of another planet which takes away the advantage of an ISRU system.

$LCH_4$ exists as an alternative to both $LH_2$ and RP-1 as it has some of the benefits of both and lacks their main downsides. As mentioned previously, $LCH_4$ has excellent ISRU capabilities but it also is relatively easy to store when compared to $LH_2$. Like RP-1, $LCH_4$ has a higher density than $LH_2$ and therefore requires smaller tanks. This generates mass savings on vehicle structures as they have to accommodate less space. Also, even if $LCH_4$ is a cryogenic fluid, it has a much higher saturation temperature than $LH_2$ (-259 °F at sea level pressure 14.7 psia) which makes it much more manageable to store for long durations of time. Since the saturation temperature of $LCH_4$ is so close to that of $LO_2$ (-297 psia at 14.7 psia), a simple bulkhead architecture can be

achieved for the complete space system. $LO_2$-$LCH_4$ propulsion systems have quite a large thrust output capability making them desirable for a wide variety of uses. Although the theoretical efficiency of a $LO_2$-$LCH_4$ propulsion system is lower than $LO_2$-$LH_2$, it's still within an acceptable range as it is larger than $LO_2$-RP-1. It's theoretical vacuum-expansion specific impulse for a chamber pressure of 1,000 psia is 369 s. [2].

#### *1.2.1.3 Non-Toxic Propellant*

The only space vehicle that has ever landed humans on the surface of other celestial bodies is the Apollo Lunar Module (LM). Six such vehicles brought a total of 12 astronauts to the surface of the moon between 1969 and 1972. The LM consisted of two stages: the descent and the ascent stage. Each of these stages had their own propulsion system. The propellant of choice for this application was a hypergolic propellant combination of nitrogen tetroxide ($N_2O_4$) and Aerozine 50. Hypergolic propellants are those which spontaneously ignite when they come in contact with one another thus eliminating the need of having an igniter. Hypergolic rocket engines by nature provide high reliability due to the way they ignite and therefore are commonly used for lander vehicle's main engines as well as reaction control engines.

Monopropellant rocket engines are another alternative that some landers have also utilized to fulfill their propulsion requirements. One example of this is the Sky Crane that was used to descend the Curiosity mars rover to the surface of Mars with the use of four hydrazine thrusters. Monopropellants release energy by chemical decomposition through the use of a catalyst and do not require an external igniter. Because of that, monopropellant rocket engines also have the advantage of providing a reliable ignition. However, they cannot provide high levels of thrust and so are often used for RCS.

Monopropellants and hypergolic propellants have the disadvantage of being highly toxic and unstable. Also, they are unsuitable for ISRU. For these reasons, an alternative that would be safer to handle while still provide reliable ignition for RCS and lander propulsion systems is desirable. $LCH_4$ is a stable propellant as it will not ignite unless properly atomized and mixed with

an oxidizer. If reliable ignition of a $LO_2$-$LCH_4$ main engine as well as a RCS is achieved, a vehicle which depends only on $LO_2$ and $LCH_4$ for its propulsion requirements can become possible. This will eliminate the need of incorporating other fluids into a space system as well as get rid of the toxicity concerns of having a monopropellant or hypergolic fluid on board.

### 1.2.2 Previous $LO_2$-$LCH_4$ Propulsion Systems

As of now there hasn't been any $LO_2$-$LCH_4$ propulsion systems flown outside of Earth's atmosphere. However, as it has been identified as an ideal propellant combination for deep space manned exploration missions, NASA has assessed different technology gaps that need to be developed for $LO_2$-$LCH_4$ propulsion systems to be used on spaceflight missions. As a result of this, NASA as well as Japanese and European space agencies have recently been developing and testing rocket engines that use these propellants for different applications [3]. Private companies such as SpaceX and Blue Origin seek to take advantage of the ISRU capabilities of $LCH_4$ as well and have been developing high thrust $LO_2$-$LCH_4$ rocket engines to be used for their launch vehicles. NASA in particular has also developed and tested a robotic lander with similar goals as those of Janus. The Morpheus lander vehicle was used to test the integration of $LO_2$-$LCH_4$ propulsion systems and has had several successful test flights.

It is very helpful to acquire knowledge from previous efforts with similar goals as those that the cSETR plans to achieve. Acting as historians and trying to understand the methodology used by previous systems tested helps to apply the lessons learned in the past into the new system that is being developed.

The following subsections will detail the endeavors of some agencies and companies in their development of $LO_2$-$LCH_4$ technologies. These technologies have been used as references for the development of the cSETR propulsion systems as well as the Janus testbed.

#### *1.2.2.1 Ascent Main Engine (AME)*

A study called the Exploration System Architecture Study (ESAS) done by NASA began in 2005 in order to address the technology required for future space exploration missions. ESAS

identified the need for a Lunar Surface Access Module (LSAM) which integrated pressure-fed reaction control and main engine $LO_2$-$LCH_4$ propulsion systems. The requirements for the Ascent Main Engine (AME) of the proposed LSAM were among others: 7,500 lbf of thrust, 355 s of vacuum $I_{sp}$ and a capability to restart 24 times [4]. To address the development of the AME, a contract was awarded to Aerojet while at the same time, NASA performed their own development activities.

Aerojet designed an ablative engine concept which when tested at sea level conditions had a lower performance than desired. However, altitude tests were performed at NASA White Sands Test Facility (WSTF) where 187 seconds of hot-fire tests were conducted using a 129:1 nozzle extension area ratio. The design was done for a 150:1 expansion ratio and so the test results needed to be extrapolated. The calculated $I_{sp}$ for these tests was of 344 s which translated to around 348 s with an expansion ratio of 150:1 [4].

**Figure 3: Aerojet $LO_2$-$LCH_4$ AME during altitude testing at WSTF [3] [4].**

NASA performed tests of their own injector concepts at NASA Marshal Space Flight Center (MSFC). The main goal of these tests was to acquire instability and performance data on a swirl coaxial injector. In parallel, NASA tested a Rocketdyne RS-18 which is a modified version of the LM Ascent Engine used during the Apollo era. Simulated altitude conditions were achieved during tests of the RS-18 at WSTF using a steam ejector. Three tests demonstrated accurate ignition at simulated altitudes between 103,000 and 122,000 ft and measurements of thrust and flowrates were done in order to calculate $I_{sp}$ performance [5].

Other tests done for rocket engines to be used on a descent or ascent vehicle included some done by Armadillo Aerospace in conjunction with NASA Johnson Space Center (JSC). A 1,500 lbf $LO_2$-$LCH_4$ rocket engine was tested under various conditions. This engine was incorporated into a VTOL-capable lander which served as a vertical testbed for it. The testbed vehicle was tested during tethered and untethered flights at sea-level conditions at Armadillo facilities in Caddo Mills, TX [6].


**Figure 4: Hot-fire test image of RS-18 vacuum ignition demonstration test. [5]**

After the sea level tests were completed the engine was taken to WSTF and was tested under simulated altitudes of up to 120,000 ft. The rocket engine was designed to have three different nozzle configurations: an under-expanded conical nozzle, an optimized bell nozzle and a dual-bell nozzle. A total of 10 hot-fire tests were conducted at the same facility that had been used to test the RS-18 in WSTF for different altitude conditions [4].

**Figure 5: Hot-fire test at WSTF of Armadillo Aerospace rocket engine under simulated altitude conditions, dual-bell nozzle installed [6].**

#### *1.2.2.2 SpaceX and Blue Origin $LO_2$-$LCH_4$ Rocket Engines*

Private companies such as SpaceX and Blue Origin have also invested in developing $LO_2$-$LCH_4$ propulsion technologies. Both companies are developing rocket engines in the 500,000 to 750,000 lbf range which can be clustered together for different launch vehicle and applications. Reusability is the main objective for both companies as they aim to decrease the cost of access to space. Both companies have achieved vertical propulsive landing of their first stages: SpaceX landing their Falcon 9 vehicle on an ocean barge from an orbital injection flight and Blue Origin landing their New Shepard vehicle from a suborbital flight. This has proven the feasibility of reusing the first stages of launch vehicles for multiple launches to different destinations. Coupled with the ability to generate $LO_2$ and $LCH_4$ on the surface of other planets, reusability would allow for the infrastructure to send humans to explore and even colonize other planets to be built.

In September of 2016, the CEO of SpaceX, Elon Musk, announced a plan for an Interplanetary Transport System (ITS). This system will implement the reusability of both a launch vehicle and a crewed space vehicle. The space vehicle is planned to have the capability of being refueled in-orbit in order to allow for the transfer burn to another planet. All of the propulsion systems intended to be used by the ITS will use an $LO_2$-$LCH_4$ propellant combination. For the first stage of the ITS launch vehicle, SpaceX plans to use a cluster of 42 Raptor engines in a sea-level configuration while the crewed space vehicle would utilize 6 Raptor engines in vacuum configuration and 3 at sea-level nozzle-expansion [7].

The Raptor rocket engine has been designed to perform under a full-flow staged combustion cycle using subcooled $LO_2$ and $LCH_4$ propellants. Some of the performance characteristics of the engine were revealed by Elon Musk on September 2016 during a presentation at the International Astronautical Congress in Guadalajara, Mexico. According to the presentation, the Raptor engine will have an $I_{sp}$ of 334 s at its sea-level expansion configuration and 382 s under vacuum expansion. Also, SpaceX claims that Raptor will operate at approximately 4,350 psi of chamber pressure and have the capability to throttle at a 5:1 ratio. With a thrust output of 685,000

lbf and 787,000 lbf at sea-level and vacuum respectively, Raptor would be one of the most powerful and efficient cryogenic rocket engines in use [7].

Since 2014, SpaceX has announced testing activities for the Raptor engine. Individual component tests were completed at NASA Stennis Space Center (SSC) in Mississippi. In order to do this the E2 test stand at SSC needed to be modified in order to provide the large flow rates of $LO_2$ and $LCH_4$ required by the tested components of the Raptor engine. In September 2016, the first test of a Raptor engine demonstrator was successfully tested in SpaceX's test facility in McGregor, TX [8].

**Figure 6: Hot-fire test of SpaceX's Raptor engine demonstrator [8].**

Blue Origin, a company based in Kent, WA, is also developing a $LO_2$-$LCH_4$ rocket engine: the BE-4. One of the goals of Blue Origin is to lower the total cost of access to space by achieving reusability of space vehicles. To do this, Blue has developed a suborbital vehicle called New Shepard which they expect to be used as a platform for space tourism. New Shepard is advertised to be able to take up to six passengers on a suborbital flight as soon as 2018.

In the past, Blue Origin has successfully completed several suborbital flights. Launching from their West Texas facility, which is near the town of Van Horn, TX and just two hours east of El Paso, Blue Origin was able to send a space capsule outside of the Karman line and return it safely back to Earth. The New Shepard's propulsion system consists of a single BE-3 $LO_2$-$LH_2$ rocket engine that produces up to 110,000 lbf of thrust.

In parallel to their New Shepard flights, Blue Origin has been in the process of developing an orbital flight vehicle. The New Glenn is expected to perform as a heavy lift vehicle that could bring payloads and astronauts to low-Earth orbit destinations and beyond [9]. In order to power

the propulsion system of the New Glenn, Blue is developing a $LO_2$-$LCH_4$ rocket engine named the BE-4.

Other than the New Glenn, the BE-4 is also a candidate to be used on the United Launch Alliance (ULA) Vulcan vehicle. Since a congressional order in 2014 that banned the use of Russian rocket engines in American space vehicles, ULA has been looking for a replacement to the Russian RD-180 rocket engine. ULA also aims to develop infrastructure for a Cis-Lunar economy for which ISRU is a must. Given that the BE-4 engine is a $LO_2$-$LCH_4$ system, it aligns with ULA's requirements and therefore has contributed to the funding of Blue Origin's BE-4 engine.

**Figure 7: Rendering of Blue Origin's BE-4 $LO_2$-LNG rocket engine [9].**

Blue Origin describes the BE-4 as using a propellant combination of $LO_2$ and liquefied natural gas (LNG). However, natural gas is mostly composed of methane and therefore it is likely that it's performance would not be affected by using pure $LCH_4$ as fuel. The BE-4 uses an oxygen-rich staged combustion cycle in order to produce as much as 550,000 lbf of thrust.

Blue Origin claims to have completed tests of the engine components such as the injector assembly and the pre-burner and date full engine tests to have begun in 2016. However, no performance results have been released from these tests.

### *1.2.2.3 NASA Project Morpheus*

NASA has developed a vehicle which is very similar to the cSETR's Janus vehicle. Morpheus is a prototype planetary lander that has the capability of VTOL. The goal of developing Morpheus was to test two key technologies. The first is the integration of $LO_2$-$LCH_4$ propulsion systems and the second is autonomous landing and hazard avoidance [10]. It's design and development started in June, 2010 at NASA Johnson Space Center and many iterations have been

done to several prototypes since. Morpheus allowed the demonstration of an integrated main engine and reaction control system (RCS) operation using the same propellant tanks to feed both propulsion systems. At the same time the Autonomous Landing and Hazard

**Figure 8: Morpheus free-flight demonstration at KSC [12].**

Avoidance Technology (ALHAT), demonstrated successful landing of an unmanned vehicle by selecting and targeting a safe landing zone.

The development of the Morpheus propulsion system was done by a NASA team also from JSC. The primary drivers for the development of this propulsion system were for it to be low cost and have fast development timelines [11]. Several versions of Morpheus' main engine have been built and tested up to date with the designated name of HD. Starting from HD1 up to HD5 modifications have been made on each iteration based on lessons learned from the testing campaign on each passing prototype.

The first engine developed to be used for Morpheus was the HD1 designed to provide 2,700 lbf of thrust. HD1 had an impinging elements injector which consisted of 132 like-impinging doublets which meant that $LCH_4$ streams collided with each other and later overlapped with the mist generated by a separate $LO_2$ stream collision. Cooling was done via fuel film cooling (FFC) which was injected trough a separate manifold in order to allow variability of FFC flowrates. The injector orifices were sized with the intent of preventing the onset of instabilities and no acoustic damping devices were incorporated to this engine [11]. The HD1 was tested twice, however, damage occurred to the injector face due to an instability detected by microphones at the test pad.

The HD2 engine was intended to be a repaired version of the HD1 however it was decided to abandon this design and proceed to HD3.

HD3 was a higher thrust engine designed to provide up to 4,200 lbf of thrust. It implemented design changes based on the failure of HD1, particularly, it included a variable position acoustic cavity ring with the goal of attempting to dampen acoustic instabilities. The engine was tested 13 times at power levels ranging from 21-60% at Armadillo Aerospace and later was tested while mounted on Morpheus which required power levels up to 72%. The testing of the engine revealed a positive outcome from the addition of the acoustic cavity ring and several harmonic modes were addressed [11].

**Figure 9: Morpheus Main Engine test at SSC [12].**

HD4 was initially designed and built to a thrust level of 4,200 lbf (later deemed HD4-A), and was flown during the first free-flight tests of Morpheus 1.5a at Kennedy Space Center (KSC). The last of these free-flights resulted in a catastrophic vehicle failure. Version 1.5b of the Morpheus vehicle was tested afterwards; however, this vehicle had a higher total mass and required a higher thrust from the main engine. To accommodate the new thrust requirement, the HD5 engine was developed and tested at SSC, yet, this engine experienced thermal issues and unstable ignitions and for this reason was never flown. Therefore, the injector of HD4-A was salvaged and attached to a "large-throat" combustion chamber which provided a maximum of 5,400 lbf of thrust. Two engines were built with this configuration and were called HD4-A-LT and HD4-B-LT of which only the former flew in the 1.5b Morpheus vehicle [12].

All rocket engines went through static tests at a test stand either at SSC or Armadillo. However, afterwards the propulsion systems were incorporated into a fully integrated Morpheus

vehicle. The integrated vehicle tests were done in three configurations: a constrained hot-fire configuration, a tethered flight configuration and a free-flight configuration. Each configuration allowed for the gradual development of the integrated vehicle. A similar approach has been followed for the development of Janus and it will be explained to detail in later chapters of this thesis.

At the hot-fire test configuration, the vehicle is completely constrained form movement by being suspended above ground using a crane and strapping the vehicle's legs to ground using chains and concrete anchors. These tests promoted the optimization of the propulsion system to the vehicle's propellant feed system as well as allowing the evaluation of the main engine's gimbal system [10].

Afterwards, a tether test configuration is used in order to study the integration of the propulsion system with the Guidance Navigation and Control (GNC) system. Under this configuration, the vehicle was also suspended 15' – 20' above the pad from a crane but free from leg constraints. This allowed for 6 degree-of-freedom (DOF) testing of the GNC without the risk of a vehicle crash. The tethered tests allowed for translation, hover and simulation landing operations [10]. After some confidence had been acquired from these tethered tests, some tethered take-off and landing tests were carried on. During these tests the vehicle was not suspended by the crane and so ran the risk of crashing into the ground. However, these tests allowed take-off and landing routines while providing range safety. After these tests were completed at JSC, Morpheus was transferred to KSC for free flight testing.

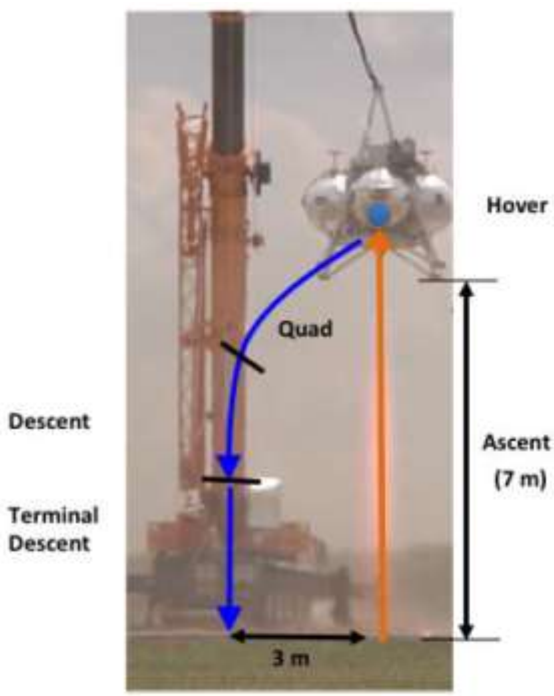

**Figure 10: Tethered take-off and landing test [10].**

The free-flight tests done at KSC focused on increasingly challenging flight profiles which included the landing of the vehicle in a 100 x 100 meter hazard field of simulated planetary terrain [10]. During these tests, Morpheus 1.5a 'Alpha' suffered a catastrophic failure resulting in vehicle loss which prompted the construction of Morpheus 1.5b 'Beta' which included the addition of the ALHAT system and later a cold helium pressurization system.

Morpheus is currently undergoing vacuum tests at NASA Glenn Research Center (GRC). At GRC's Plum Brook facility the Spacecraft Propulsion Research Facility (B-2) has been recently upgraded to allow tests of next generation upper stages and Morpheus took advantage of this to test the vehicle at simulated space conditions.

The Morpheus project has been used as a baseline for the planning and integration of Janus. Due to the similarity of the goal at hand, following on the lessons learned and the approach used by the NASA team in charge of Morpheus helped to define an overall scope for Janus. Several of the students involved in the Janus project have had the opportunity to intern at JSC and experience the firsthand the Morpheus project. That, coupled with the constant mentoring from engineers at JSC has allowed for a helpful transfer of knowledge and information to benefit the development of Janus at the cSETR. The transfer of hardware specifically the propellant tanks and the propulsion system has also been considered, however, as it will be further explained in later chapters, some characteristics of Janus has made it impractical to use Morpheus hardware. Nevertheless, the design of some components and fluid systems have emulated those of Morpheus.

# Chapter 2: Janus System Overview and Project Planning

## 2.1 Vehicle Objectives

The cSETR aims (among other goals) to contribute in the development of $LO_2$-$LCH_4$ technologies. For this, since the center's inception, several projects involving $LO_2$-$LCH_4$ have been pursued. Some of the $LO_2$-$LCH_4$ technologies that have been completed or are currently under development at the cSETR are:

- A torch igniter with a swirl-coaxial injector using $LO_2$-$LCH_4$ as propellants. This igniter was designed built and tested at the cSETR and a patent was filled for it.
- A reaction control engine (RCE) called the Pencil thruster that uses $LO_2$-$LCH_4$ propellants. This engine comes in two configurations: a 5 lbf sea-level RCE and an 8 lbf vacuum-expanded RCE. Design and manufacturing for this engine has been completed and testing is occurring at the time that this thesis is being written.
- A 500 lbf rocket engine with a pintle injector that can throttle in steps down to 125 lbf named the Centennial Restartable Oxygen Methane Engine (CROME). This engine is in its final stages of design and is scheduled to be tested in August, 2017.
- A larger version of the CROME engine called CROME-X. This rocket engine utilizes and is capable of producing a thrust output of maximum 2,000 lbf while being able to throttle down to 500 lbf. In parallel to the CROME engine, the CROME-X is being developed and is scheduled to be tested after CROME.

These different technologies would each serve different purposes when integrated into a vehicle. Since they all operate using the same propellant combination it becomes possible for them to be fed using common propellant tanks. Janus has been envisioned with this idea in mind and therefore it will serve as a testbed for the simultaneous application of these in-house developed technologies.

The cSETR was awarded the MUREP Institutional Research Opportunity (MIRO) grant as part of NASA's Minority University Research and Education Project (MUREP). This 5-year grant

will last until the end of July, 2020 and has allowed for the pursuit of several research projects; among them is Janus.

Janus is a fully autonomous vehicle that has the capability to perform a vertical take-off and landing (VTOL) maneuver. From the technologies listed above, Janus will incorporate the use of the swirl-coaxial torch igniter in order to ignite the CROME-X rocket engine, which will be implemented as its main propulsion source. Furthermore, the vehicle will incorporate a set of Pencil thrusters at their sea-level configuration for its reaction control system (RCS).

These incorporated technologies have different operating conditions and therefore require to be provided with fluids at different conditions particularly of flow rates and pressures. Since none of the individual components have a way of pressurizing the propellants to their operational conditions, the vehicle must be able to accommodate for the requirements of each. Janus will achieve this through a pressure-fed system by having pressurized tanks which will be kept at a constant pressure by the use of a pressurizing inert gas such as helium (He) or Nitrogen ($GN_2$).

Janus is also intended to include components that have been additively manufactured at the UTEP W.M. Keck Center for 3D Innovation. 3D printing components allows for rapid prototyping during their development phase. Also, 3D printing makes it possible to manufacture complex geometries as a single solid part as opposed to having to be machined as different parts and then joined by means of welding or bolting. Although many advances have been made to additive manufacturing of metallic parts, it's still a discipline that requires research to be done. Incorporating additively manufactured components to Janus will serve as a demonstration for the feasibility and benefits of having 3D printed components in a flight vehicle.

Another technology that is intended to be included in this robotic lander is the use of a methane solid oxide fuel cell (SOFC). A SOFC is a device that would allow the extraction of electrical power from a chemical reaction. Every space vehicle uses two main consumables: propellants and electricity. An SOFC makes it possible to generate electricity by using the propellants on board the vehicle. The idea is that by means of a chemical reaction between the $LO_2$ and $LCH_4$ that are used for the propulsion systems, electricity can be generated. This provides the

significant advantage of generating on-demand power required by the vehicle as long as there is a readily available supply of propellants. Development of the methane SOFC required to power Janus' components has not yet started at the cSETR. For this reason, the initial prototypes of Janus are not planned to include the SOFC as a mean of providing power. However, it is expected that a team dedicated to the development of this methane SOFC will be created in order for it to be incorporated to the final flight version of the vehicle.

### 2.2 Flight Profile

In order to begin the conceptual design of the Janus system, a final flight mission had to be established. The mission for Janus was defined as a short duration flight during which all of the incorporated systems could be demonstrated in parallel. Janus in its final configuration must be able to demonstrate the use of its propulsion system which entails firing all its engines (CROME-X and set of Pencil thrusters) at their thrust capabilities while maintaining dynamic control [13].

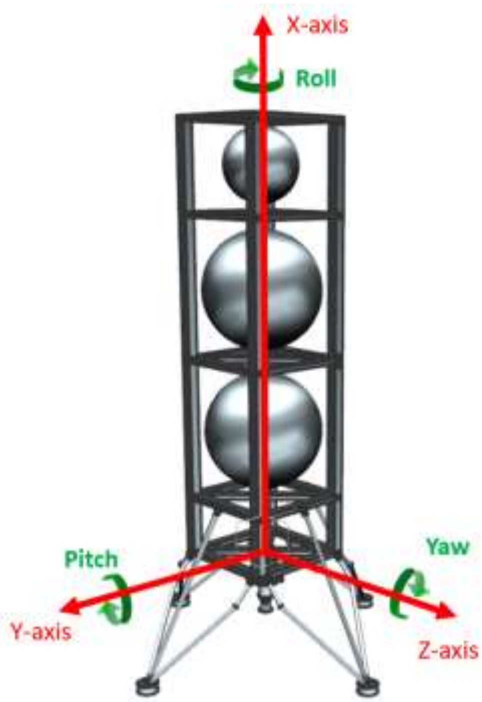


**Figure 11: Janus vehicle coordinate frame.**

It was decided, as it will be further explained later in this text, that the vehicle must be controlled by the use of the throttling capabilities of the CROME-X main engine for its vertical translation. The CROME-X engine will also be incorporated with the use of a gimbal system which will allow for the dynamic control of the vehicle's pitch and yaw rotational motion. Figure 11 shows the vehicle coordinate frame as well as its rotational degrees of freedom (DOF) labels. It is evident from this rendering that the pitch and yaw axis are symmetrical as is often the case in space vehicles. Furthermore, the incorporation of the gimbal system also allows the capability for controlled horizontal motion; however, it was determined that a horizontal translation during the flight of

Janus would be unnecessary as it would only add complexity to the control algorithm without providing any additional value to the demonstration of the integrated propulsion systems which is the main goal of this vehicle. Lastly, the use of the Pencil RCE will be incorporated through control of the roll rotation of the vehicle. A predetermined number of RCEs will be attached to the vertical beams of the Janus' structure in coupled pairs. A minimum of four pencil thrusters are required to control this motion; however, the total number of engines must be determined based on the vehicle's geometry and mass (mass moment of inertia), the moment arm and thrust of the RCE, and the minimum time required to perform a roll maneuver.

The flight of the vehicle has been selected to be done solely as a vertical take-off and landing maneuver. Janus will therefore perform a vertical ascent up to an altitude of 20 ft. where it will hover for a duration of 10 s and perform a roll maneuver. The roll maneuver will be done using the RCS making the vehicle do a 360° turn. Afterwards, the vehicle will begin a controlled descent towards a soft vertical landing.

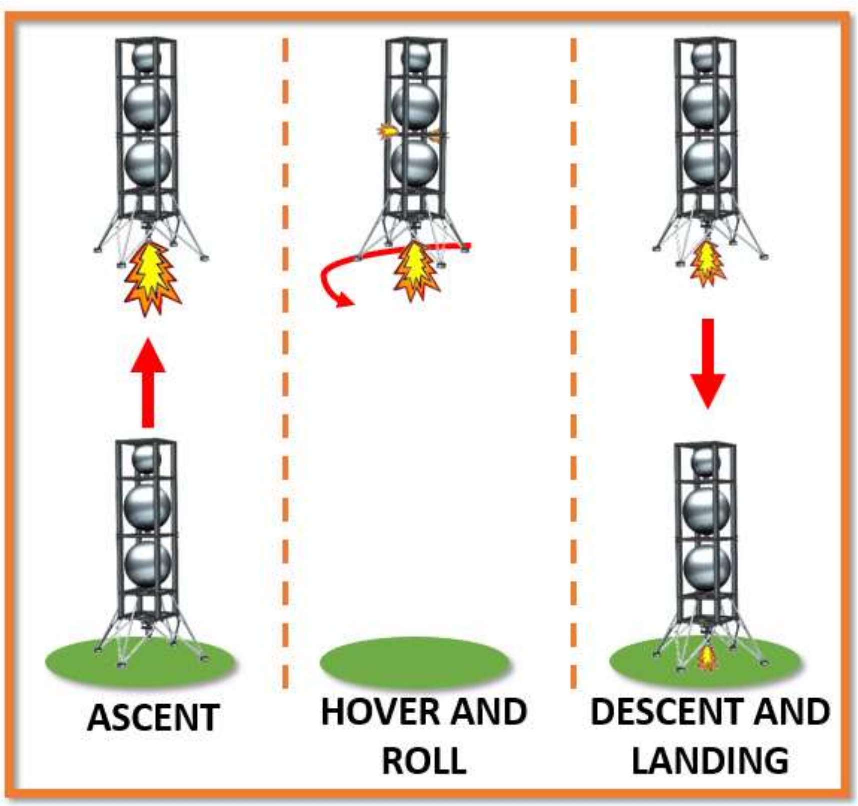


**Figure 12: Janus conceptual flight profile.**

As pictured in Figure 12, the mission profile consists mainly of three stages as described below: (Notes: Mission times are calculated approximations and are written in the commonly used rocketry countdown notation e.g. T + 05s denotes 5 seconds after ignition. Accelerations during the flight are referenced in g's as an accelerometer would sense them if mounted on the vehicle.)

1. Ascent Stage (T +00s – T +12s):
    a) At T + 00s the CROME-X main engine will be ignited and throttled from zero to a thrust level corresponding to 50% of the vehicle's launch weight. This will be an idle thrust state at which the vehicle will not liftoff yet. Having this idle thrust state allows for the verification of stable ignition and engine health prior to liftoff. It would also provide enough time to shut down the mission while the vehicle is still on the ground in the case that any red-lines from the automated sequence are triggered during engine ignition [12].
    b) At T +05s, if the main engine's performance is deemed nominal, the CROME-X will be throttled to a thrust level equivalent to a vertical acceleration of 1.05g. As the vehicle loses mass due to the burning of propellant, the engine throttle must be adjusted in such a way that a steady acceleration is achieved. This relatively low acceleration would maintain structural loads at a minimum and allow for a steady ascent. At this point, the GNC system will maintain the vehicle in its upright vertical orientation by correcting any misalignment using both CROME-X's throttle and the gimbal system.
    c) After the vehicle has ascended to a height of approximately 10 ft. (half as much as the maximum expected flight altitude), which is expected to occur at approximately T +08s, the main engine will be throttled down in order for the vehicle to decelerate. The throttle should be gradually lowered as the vehicle weight decays such that a constant deceleration rate of approximately 0.95g is achieved. At this rate, the vertical velocity of the vehicle will fall to 0 ft./s at around T +12s and an altitude of 20 ft. will have been reached. Throughout this stage of the flight, any deviation in the vehicle's orientation

will be corrected by the GNC through the combined use of the throttle and gimbal system.

2. Hover and Roll Maneuver Stage (T +12s – T +22s):
    a) Once the desired altitude of 20 ft. has been achieved and all vertical velocity has been eliminated, the CROME-X engine will be throttled back up to match the weight of Janus; effectively achieving a vertical acceleration of 1g. At this point the vehicle will be motionless and hovering in the air. The throttle of the main engine must be actively adjusted during this stage in order to match the thrust level to the decreasing weight of the vehicle. A stable hover should be achieved within 1 second of arriving at the desired altitude.
    b) At T +13s, the roll maneuver will commence. The RCS will be activated in order for the vehicle to perform a 360° turn about the x-axis. The roll maneuver should be completed in two burns of the RCS: The first burn will provide angular momentum to the vehicle making it start turning. The second burn must counter the first burn and negate all angular momentum and stop the rotation of the vehicle. This maneuver will take place while Janus is still hovering at 20 ft. and any anomalies in the symmetry of the RCS firings will be adjusted by the control of the main engine gimbal and thrust. The roll maneuver must be completed within 8 seconds (at T +21s), however, an extra second of hover time is allotted in the case that any further adjustments are necessary.
3. Descent Stage (T +22s – T +32s):
    a) At T +22s the descent stage will begin. The main engine will be throttled down to an acceleration of 0.95g. The vehicle will begin to accelerate towards Earth. This process must be controlled by the use of the main engine throttle in order to achieve a constant rate of acceleration.
    b) At approximately T +25s, once Janus has descended to a height of around 11.5 ft. (halfway between the maximum height of the flight and the final landing-hover altitude of 2 ft.), the throttle of the main engine is increased in order to slow down the descent

of the vehicle. The CROME-X should output a thrust equivalent to an acceleration of 1.05g. At this rate, the vertical velocity of the vehicle will be 0 ft./s at T +28s and an altitude of 2 ft.

c) After reaching a vertical velocity of 0 ft./s, the main engine throttle will be lowered to match the weight of the vehicle and manage a hover. This hover will be held for 2 seconds from T +28s to T +30s; the purpose of it being to allow the GNC to level the vehicle preparing it for a final descent to ground.

d) At T +30s the engine will once more be throttled down to a thrust level corresponding to an acceleration of 0.95g. Consequently, the vehicle will begin to descend until it touches ground at approximately T +32s. Given that the vehicle is lowered at a rate of 0.95g the vertical velocity at the time of touchdown will be approximately 3 ft./s in the negative x direction. At this velocity, the impact force of the landing is relatively low and easy to dissipate, minimizing the structural loadings associated with it.

e) Once the vehicle has landed, the main engine will be shut down. At this point the mission will have been completed after an approximated flight duration of 32 seconds.

The flight profile described above is a conceptual mission through which the goals of the vehicle can be achieved. Some values for this flight profile were selected arbitrarily while keeping the end-goals of the testbed in mind. For example, the maximum flight height of the vehicle does not need to be limited to 20 ft. and the same can be said of limiting the acceleration loads to the g values specified above. However, this profile serves as a robust guideline for the preliminary sizing of some of the sub-systems of the vehicle. This allows for the flexibility of changing the flight profile in the future within reason. Having an approximation of what the propulsion requirements for the fight of Janus is also necessary to develop test matrices for the vehicle components during their testing campaigns.

A script was generated using MATLAB in order to calculate some of the characteristics and timing of the mission. The plot shown in Figure 13 traces the estimated altitude that the vehicle will fly at over the time of the mission as described above. This calculation assumes a constant

acceleration and deceleration during ascent and descent; and an exact hold time of the hovering maneuvers.

One consideration to make during the flight of a space vehicle is the fact that the propulsion

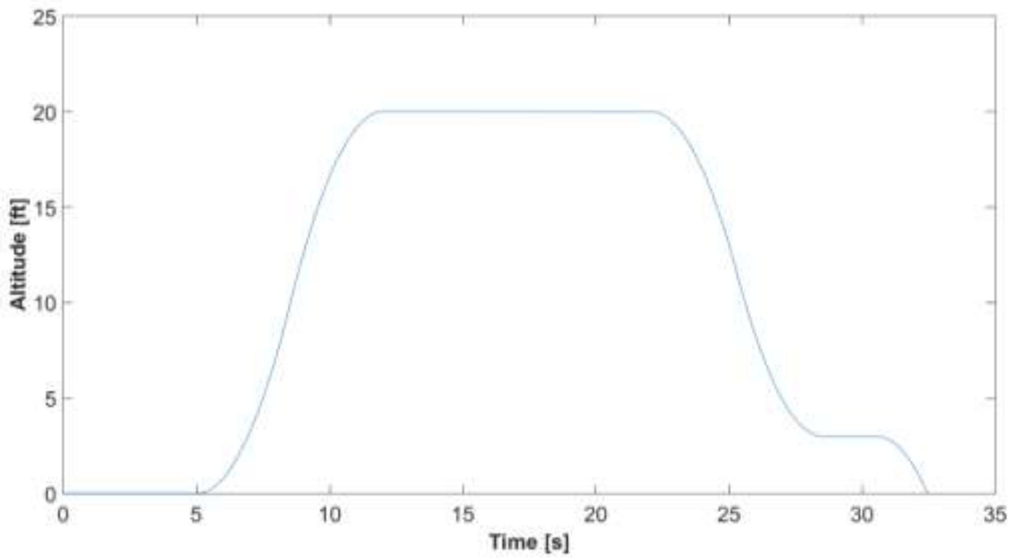


**Figure 13: Janus flight altitude over time.**

system consumes a lot of propellant while it is firing. This means that the total weight of the vehicle is decreasing during its flight. Therefore, the mass loss of Janus was approximated using the same MATLAB model. It is evident from Figure 14 that the rate of weight loss changes at different stages of the flight profile (i.e. from the idle thrust state to the ascent stage to the hover stage). Although the values for this change in mass would vary depending on the initial take-off weight of the vehicle, the results shown in the following figures are normalized. Once an estimation of the initial weight of the vehicle is known however, this calculation can be used to determine the total amount of propellant that the mission requires and also size the propellant tanks. This will be done through an iterative process since a change in the vehicle mass renders a change in the amount of propellant necessary which in turn alters the initial vehicle mass and so on.

Another aspect that was calculated is the thrust required by the main engine as a function

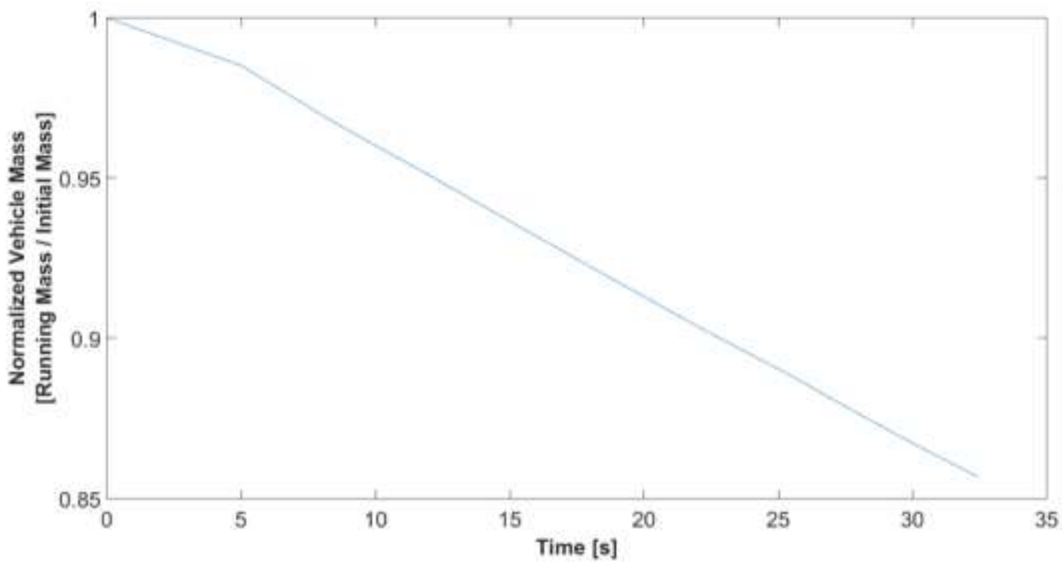


**Figure 14: Normalized vehicle mass as it drops over time.**

of time throughout the flight. Assuming an instantaneous response time on the thrust of the main engine, Figure 15 shows the calculation of the thrust required from CROME-X in order to perform the different stages of the flight. Theoretical data gathered from the design calculations of the main

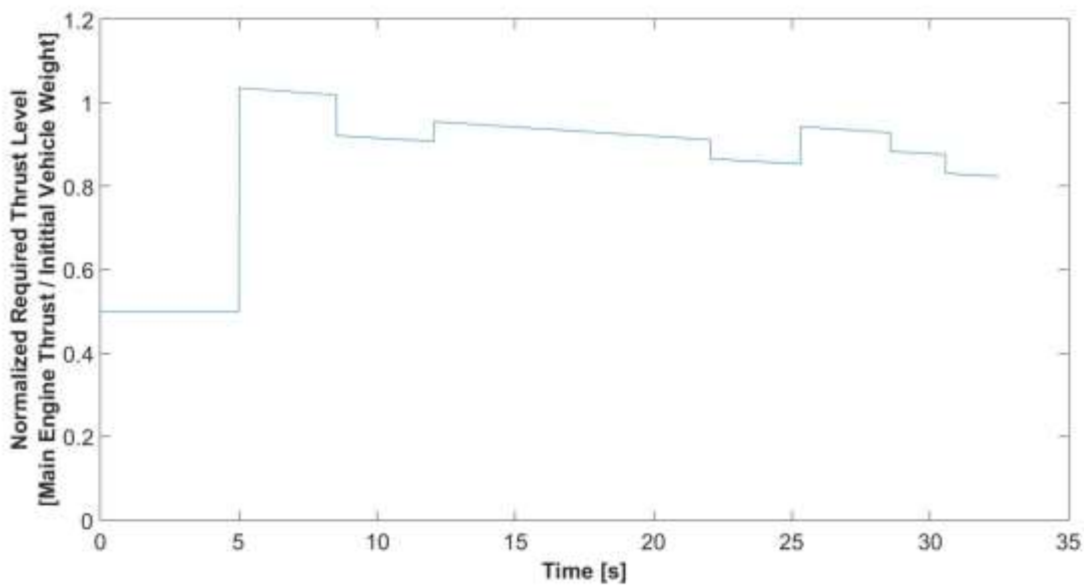


**Figure 15: Required thrust level (normalized over initial weight) over time.**

engine give a correlation between thrust level and propellant weight flow rate required. By

coupling that data to the thrust level required by the vehicle, an approximation of the weight loss throughout the flight could be made.

### 2.3 Project Planning

The development of Janus has been possible thanks to the NASA MIRO grant awarded to the cSETR. The grant started in August, 2015 and it is to last until August, 2020. This timeline was used as a base to establish the timeline to be followed for the development of both the Janus and Daedalus vehicles.

In order to simplify the process of the development of Janus, the project was subdivided into three major prototypes on which the components of the vehicle will be implemented gradually. Each prototype will incorporate new systems and improve upon its predecessor approaching specific milestones in a systematic way. This process will facilitate the design process and maintain focus on short-term goals [13].

Given the nature of the cSETR as an academic research institution, the constant student turnover becomes an issue to long duration projects such as is Janus. Every semester, students that work at the cSETR graduate and new hires need to be familiarized and trained into the current projects. Splitting this long project into smaller duration prototypes, allows students to focus on a specific goal and aim for its completion before their graduation. Consequently, it becomes imperative that the progress and lessons learned by each student is formally documented and shared with the rest of the team. A platform to facilitate this was implemented in the form of a secure repository of files called TortoiseSVN. The SVN system functions as a cloud-based storage of all the files related to the development of Janus and its components. Only the people involved in the project are allowed to access these files and a version control system provides a secure way of sharing information and relaying it to new generations of the team.

#### 2.3.1 Prototype Goal Definition

The three different prototypes of Janus follow a similar progression to the way NASA approached the development of the Morpheus lander. First, a static configuration will be tested

and deemed J-1. Afterwards, in the J-2 prototype, the vehicle will hang from a crane and will be tested in a tethered configuration avoiding the risk of vehicle crash. The final prototype, J-3, will be an autonomous flight version of the vehicle which will incorporate all the $LO_2$-$LCH_4$ technologies intended to be tested. Figure 16 illustrates the progression of the prototypes toward a flight vehicle.

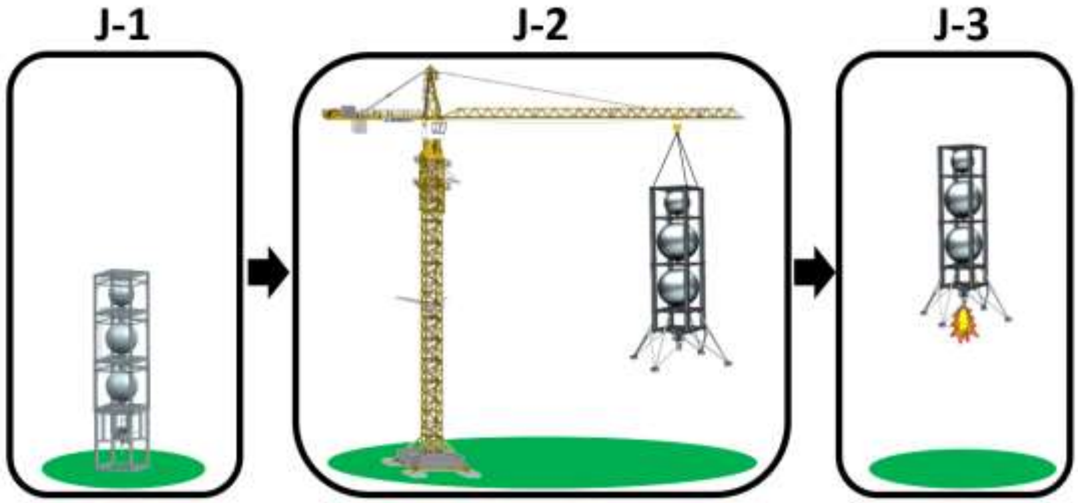


**Figure 14: Janus prototypes: Static (J-1), Tethered (J-2) and Autonomous (J-3).**

### *2.3.1.1 J-1 Prototype*

The J-1 prototype will be the first iteration of the Janus vehicle to be built and current efforts are in the development of this prototype. The purpose of this prototype is to act as a static testbed on which the performance of the propulsion systems will be assessed. The development and testing of J-1 will also be a training ground on cryogenic rocket engine test stands for the students involved.

This prototype will include the CROME-X and Pencil thruster propulsion systems as well as all the instrumentation and feed lines required for their testing; despite that, the test tanks and structures to be used during this prototype will not be flight-ready. Rather, they will be heavy and robust versions in order to reduce the risk of failure while an understanding of the performance of the propulsion systems is achieved. Also, J-1 will be lacking some of the subsystems that are expected to be included in the flight vehicle. That is: the main engine will be tested without a

gimbal system, the landing gear will not be included to the structure of the vehicle, there will not be an integrated GNC computer on the vehicle, and the electrical power will come from batteries rather than the solid oxide fuel cell (SOFC).

J-1 itself will be split into two developmental stages: J-1a and J-1b. J-1a will perform solely as a test stand for the CROME-X main engine, whereas J-1b will be used to test a static version of Janus implementing several of the different technologies to be demonstrated in a vehicle-like configuration. Having these different configurations of J-1 became necessary given that the CROME-X engine is an in-house developed engine and testing for its performance needs to occur. Testing a cryogenic rocket engine requires the capability to do several things like: measuring the thrust that is being produced, the propellant flowrates that are flowing into the test article, flexibility in the test duration and conditions, etc. Having this capability becomes problematic or even impossible to have when the engine is being tested attached to a vehicle. Thus, the need for a facility dedicated to test the CROME-X engine arises.

An option that was considered was to contract the testing of the engine at an outside facility such as NASA WSTF or even SSC. This, however, becomes impractical due to its expense as well as the need to travel. Consequently, it was decided that the engine will be tested in-house. The cSETR currently does not have the capability of testing a 2,000 lbf $LO_2$-$LCH_4$ rocket engine. However, with the acquisition of the Technology Research and Innovation Acceleration Park (tRIAc) in Fabens, TX, it became possible to build a facility to test the CROME and CROME-X rocket engines.

The goal of the J-1a prototype is to test the main engine propulsion system by itself. At the end of the test campaign of J-1a the following will be known of the CROME-X:

- The specific impulse ($I_{sp}$) at various conditions.
    - At different thrust levels ranging between 2,000 lbf and 500 lbf.
    - At different mixture rations (MR).
- The controllability and response time of the throttle.
- The optimal amount of cooling required.

- Dampening instabilities (if necessary).
- Performance during a simulated Janus flight profile or mission duty cycle (MDC).

Once the performance characteristics of the CROME-X rocket engine have been reviewed, J-1a will be reconfigured into J-1b. The J-1b prototype will use the same support structure employed by J-1a, however, the capability to measure thrust will be removed and the prototype will be built to resemble the configuration that will be used for the flight vehicle.

J-1b will follow the basic architecture intended for how Janus will look. Tanks will be stacked in a vehicle configuration and the Pencil RCE will be added to the system. The purpose of J-1b is to simulate the configuration that will be used for the flight vehicle as closely as possible. Although most of the components will not be rated for flight by this point (i.e. tanks and structures will be heavy versions), it is intended that the flow systems are implemented as they are envisioned on the flight vehicle. The J-1b configuration will allow the following:

- Evaluate the performance of the parallel operation of the RCS and main engine.
- Characterize the performance of the propulsion systems under flight-like propellant feed system conditions.
- Simulate Janus MDC including the use of the RCS.

During the test campaign covering the J-1 prototype, the procedures and protocols to be followed by all subsequent prototypes will be developed. As it will be explained later in this text, many of the difficulties that arise from the handling of cryogenic fluids can be overcome by the establishment of procedures. J-1 will serve as a learning ground to implement these procedures having a relatively lower capacity for catastrophic failure.

Given the similarity of the two projects at this stage of their development, the J1 infrastructure will be shared between Janus and Daedalus. The CROME engine (used as Daedalus' main engine) will therefore be tested on the same J-1a test stand and the integrated operation of Daedalus will be tested in a similar way as J-1b.

#### *2.3.1.2 J-2 Prototype*

The J-2 prototype is intended to introduce some of the flight-ready components to be used on Janus as well as control mechanisms to be used during flight. In a similar fashion to what NASA did during the development of the Morpheus lander, the J-2 prototype will consist of suspending the vehicle from a crane and testing the propulsion systems and GNC while it is hanging. This type of testing will be referred to as a tethered test.

J-2 will introduce the development of most of Janus' flight systems. The heavy test tanks that will be used for the J-1 prototype will be swapped for light versions and possibly so will be the structures and feed lines. Also, a landing gear will be added to the structure. However, most importantly, the J-2 prototype will see the implementation of the main engine gimbal as well as the GNC system. The SOFC will be developed parallel to the construction and testing of this prototype. In the case that the SOFC is finished by the time that the J-2 prototype is being tested it can be included into the tethered test campaign, nonetheless it is not required by J-2 as it can be powered by batteries as was J-1.

The test campaign of J-2 will include different configurations. Initially Janus will not only be suspended from a crane but it will also be restrained from movement by securing it to the ground with the use of chains. This configuration will allow the test of the propulsion system with the flight hardware integrated to it. At the same time, the performance of the gimbal will be evaluated while the CROME-X is being fired. Testing of the gimbal system is not possible under the J-1 prototype because of the risk of damaging the test stand. The J-2 configuration does not pose this risk since the vehicle will be hanging a good distance from the ground.

After the gimbal has been evaluated, the ground restraints will be removed but the vehicle will still be tethered to the crane. Under this configuration, the first integrated tests of the GNC will take place. While suspended from the crane, the vehicle will perform ascent hover and descent maneuvers using the GNC system. Instrumentation will be used to detect the vehicle's motions and this information will be used by the GNC to send signals to the main engine's throttle and gimbal mechanisms in order to control those vehicle motions. In the event of failure to control the

vehicle, the main engine will be shut down and the vehicle will fall and hang from the tether avoiding a collision with the ground.

The vehicle's landing gear will also be tested during the J-2 prototype's test campaign. Having the vehicle suspended from a crane allows for a controlled descent rate without the use of the main engine. The vehicle should be lowered at different rates in order to validate the performance of the landing legs in absorbing the landing loads.

Once the J-2 test campaign is completed, the following goals will have been achieved:

- Understand the behavior of the gimbal system at different thrust levels.
- Controlled flight via GNC system.
- Developed telemetry systems for flight vehicle.
- Test integrity and performance of landing gear (legs).

***2.3.1.3 J-3 Prototype***

The final prototype will be J-3. This prototype consists of Janus performing a free flight test of its VTOL flight profile. The vehicle will be arranged in the same way as J-2 with the addition of the SOFC in the case that it hasn't been incorporated already. Under this configuration, however, the crane will be removed and the vehicle will be free to fly autonomously.

The testing done under the previous prototypes will provide with a robust base of knowledge that will enable the autonomous flight to take place. The incremental approach that will be taken shall allow the team to become proficient in handling the separate systems that make up Janus and how they interact with one another.

The main goal of the J-3 prototype will be to perform the aforementioned flight-profile. However, the initial flights without the crane for protection might be carried out at a lower altitude and progressively increase to the proposed altitude of 20 ft. Afterwards, in the case that the flight tanks have enough volume to contain larger quantities of propellant, the mission may be modified to include a more ambitious flight-profile. Performing the automated flight of Janus at its J-3 prototype configuration will deem the Janus project a success.

### 2.3.2 Top-Level Timeline

The timeline for the development of the Janus vehicle was based on the duration of the MUREP grant mentioned earlier. The project started on the same year that the grant was awarded to the cSETR and its expected to be completed by the end of 2020 by which time the MUREP grant will be coming to an end.

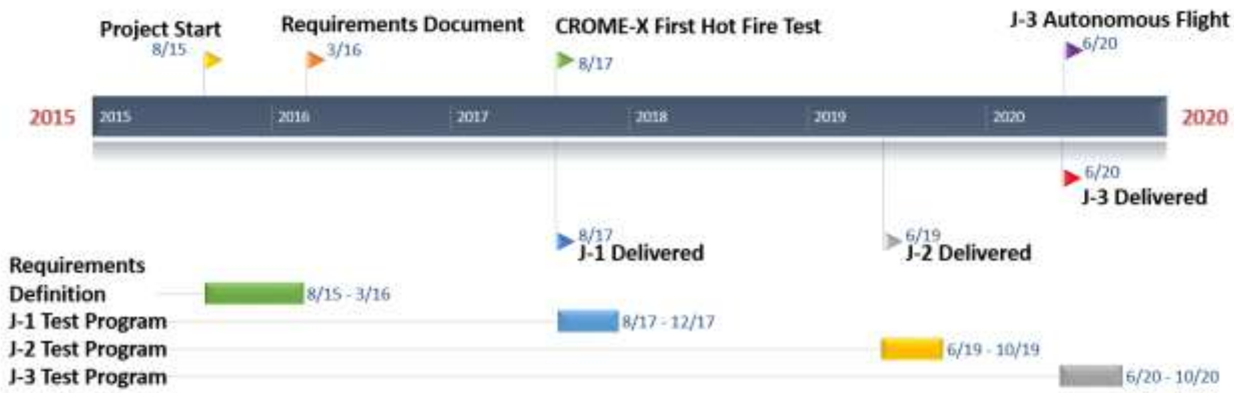


**Figure 15: Janus Timeline**

Figure 17 depicts the timeline that was generated for the development of Janus. The project officially started in August, 2015; after that some time was allocated for the clarification of the vehicle's goals and requirements. This process included the definition of the different subsystems that would be included to the vehicle as well as the flight-profile to be completed by it. It was around this time that it was decided to approach the development of Janus by the use of prototypes. By March, 2016 this process was completed and an initial requirements document was developed. However, as the system evolved, some changes have been made. Given that the requirements may continue to change in the future, it is important to say that the developments mentioned in this thesis align with the goals and requirements as of May, 2017.

With the requirements defined, a deadline was established for each of the different prototypes. The J-1 prototype is expected to be completed by the end of the summer of 2017. Setting up this prototype, however, relies on the construction of the tRIAc facility. Although the tRIAc park has been scheduled to break ground on April, 2017, some delays have been experienced which in turn may delay the fabrication of the test stand required for J-1. Be that as it may, the

testing of the J-1 prototype and therefore the first hot-fire test of the CROME-X engine has been scheduled for August, 2017 and it is to have a test campaign spanning the rest of the year.

A gap of approximately a year and a half has been allocated between the completion of the J-1 test campaign and the deadline for delivery of the J-2 prototype. Flight-ready versions of many of the systems required will need to be developed and manufactured, nonetheless, the experience acquired from the development of the J-1 prototype should enable a speedy transition into flight hardware. The test campaign for the J-2 prototype is scheduled to take place starting June, 2019 and extend until the end of that year.

A shorter period has been allocated for the development of the J-3 prototype following the test campaign of J-2. By this point the vehicle will already have incorporated most flight hardware; therefore, the assigned year between J-2 and J-3 will be filled with the work required by any modifications of the tRIAc facility. Also, the test campaign for J-2 might take longer than the time allotted given the complexity of the systems tested. This schedule leaves enough time for any extensions required. The J-3 prototype is expected to be delivered by June, 2020 and all the autonomous flights should take place by the end of that year.

### 2.4 Subsystem Definition

To begin the integration of the Janus vehicle it was necessary to define each individual subsystem that would be included into it and what their specific role would be. During the definition of the subsystem, components must be assigned to each one, clear interface points must be determined, and requirements must be assigned to them. By clearly defining the interfaces and components belonging to each subsystem, the team assigned to the development of it will have an explicit understanding of what their responsibilities are.

It has been established that the vehicle integration will be done in a modular fashion. This approach allows the individual design of modules that can be swapped in and out of the vehicle. A module has been assigned to each of the mayor subsystems of the vehicle and the interfaces of each subsystem is defined through its module. However, some of the subsystems such as the

propellant feed and the structures must take part in several of the different modules. Also, some of the modules contain more than a single subsystem. The modules will be explained to detail later in this text but the subsystems will be defined below.

### 2.4.1 CROME-X Main Engine

The CROME-X main engine is one of the most important systems in the vehicle as well as being the most complicated of them all. Given that it will be utilized for a lander vehicle, it requires deep throttling as well as gimbal control. To fulfill those requirements this engine will be able to throttle from 2,000 lbf to 500 lbf of thrust and accommodate a gimbal system. The development of this engine helps to fill a $LO_2$-$LCH_4$ technology gap the same way that the HD engine from the Morpheus project does. The development of this engine began a couple of years before the MUREP grant was awarded to the cSETR. However, since a facility for hot-fire testing an engine of such size wasn't available at the time, little focus was given to its development until the grant was awarded and the plans for both Janus and tRIAc were devised. Therefore, the project for CROME-X officially started towards the end of August, 2015.

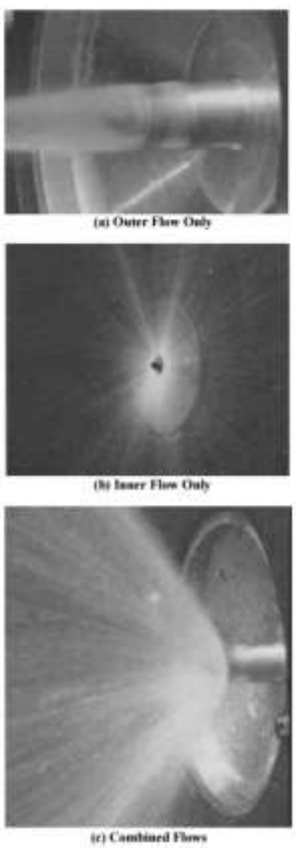


**Figure 16: Pintle injector flow [14].**

The first iteration of the CROME-X engine is intended to use a pintle injector with additional orifices along the injector face to provide fuel film cooling (FFC) of the combustion chamber. This type injector works by colliding an annular flow of one of the propellants against a radial flow of the other propellant effectively creating a cone of mixed and atomized propellants as shown in Figure 18.

This type of injector was selected because of the benefits attributed to it in literature. One of such benefits is the fact that it has been proven to be scalable to a wide range of thrust levels without the onset of combustion stabilities making it ideal for throttleable operations [14]. The scalability of it also facilitates the parallel design of both the CROME-X

2,000 lbf and the CROME 500 lbf rocket engines and for this reason both engines will use the same basic pintle injector design. Pintle injectors have also demonstrated the ability of delivering high combustion performance measured using the characteristic exhaust velocity (C*). Pintle Injectors typically yield 96-99% of theoretical C* values [14].

For future iterations of CROME-X, in order to reduce or even eliminate FFC, it is intended to make a regeneratively cooled combustion chamber. The concept of a regeneratively cooled rocket engine consists of flowing one of the propellants through channels going around the combustion chamber and nozzle effectively creating a heat exchanger that would cool the engine components. Doing this with cryogenic propellants such as $LO_2$-$LCH_4$ becomes difficult given the low boiling temperatures of this fluids especially operating under a pressure-fed system like Janus. Because of this, the propellant being injected would be in its gaseous phase. A pintle injector requires both propellants to be liquids; therefore, the regeneratively cooled CROME-X engine will need to operate using a different injector concept. To satisfy this, a shear coaxial injector was devised. With this injector concept, a liquid stream of a $LO_2$ is injected normal to the face of the injector; around it, an annular flow of gaseous $LCH_4$ (vaporized by the regenerative cooling channels) is injected coaxially. The gaseous flow therefore atomizes the liquid flow and creates a combustible mixture in the process.

Although the concept for the shear-coaxial injector was established, the development of it was put on standby in order to prioritize the development of the pintle injector for the initial engine iteration. Nonetheless, characterization of the capabilities of $LCH_4$ to be used for a regenerative cooled engine is currently being done using a high heat flux test facility (HHFTF) at the cSETR Goddard Combustion and Propulsion Research Facility. The tests done at the HHFTF are being carried out in parallel to the development of the current pintle injector and FFC CROME-X engine.

The CROME-X engine shall be delivered in a package that can be integrated to the vehicle as a module. This package will include the main throttleable valves, all instrumentation required for its operation, the $O_2$-$CH_4$ torch igniter and its valves, and a structure to hold everything in place.

### 2.4.2 Torch Igniter

A lander vehicle must be able to start its main engine as many times as necessary on command. In order to do this, many methods are commonly used for ignition such as pyrotechnics or hypergolic fluids. To make a fully integrated $LO_2$-$LCH_4$ vehicle that doesn't require many different fluids to operate, a torch igniter was designed at the cSETR. The idea of a torch igniter is that it can utilize small amounts of the same propellants as the main engine, ignite them with a spark plug and create a flame that can be used to ignite the propellants in the main engine. A method like this has been utilized in the past for engines such as the SSME.

The cSETR $O_2$-$CH_4$ torch igniter has completed many hot fire tests; the latest ones having being done in late 2016. It will be the ignition method for both the CROME and the CROME-X main engines. 100% ignition rate was achieved with the use of gaseous propellants, however, less than optimal reliability was experienced when using liquid propellants. The propellant going into the igniter must therefore be carefully conditioned to the point where reliable ignition is achievable.

This igniter contains a swirl coaxial injector. The oxygen is introduced through an axial orifice while the methane is injected in a tangential swirl pattern around the combustion chamber. The propellants are mixed due to the viscous shear generated between the two flows and the mixture is then ignited with the use of a spark plug.

The torch igniter includes two solenoid valves that are used to control the flow going into it. In order to integrate it to the CROME-X engine, structural supports must be provided for the igniter as well as its valves. The only instrumentation necessary for the operation of the igniter is a pressure transducer placed at the chamber and used to verify whether or not it has successfully ignited. However, for the initial tests of the vehicle it might be necessary to also measure the quality of the propellant going into the igniter and therefore additional instrumentation would be required.

### 2.4.3 Reaction Control Engines (RCE)

The reaction control engines are the secondary source of propulsion for the Janus vehicle. Although they will only be used for roll control of the vehicle, it is imperative that they provide reliable ignition in order to effectively perform the roll maneuver.

An RCE was developed by NASA to be used on their Morpheus vehicle. This thruster was designed based on a converted torch igniter from an Aerojet engine [15, 16]. The design was given to the cSETR and modifications to it have been made with the goal of increasing its performance. This thruster has been named the Pencil engine by the cSETR and testing is currently being done at the Goddard Combustion and Propulsion Research Facility under its sea-level configuration.

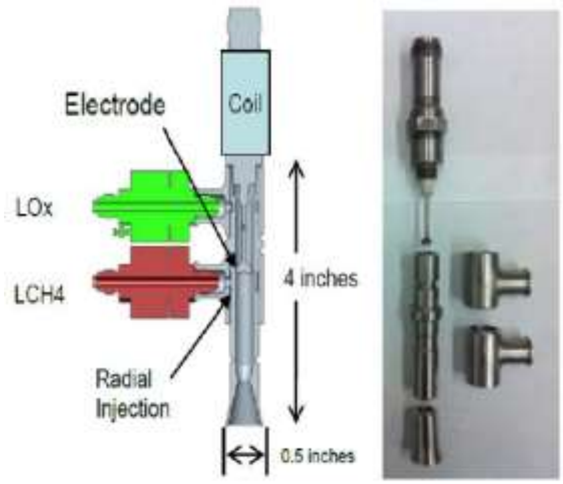


**Figure 17: Initial NASA design of RCS [16].**

Although similar in nature to the torch igniter, this engine is capable of providing 5 lbf of thrust at sea level. The method of injection is based on like-impinging elements going across the combustion chamber and being ignited with a modified spark plug. The valves used for propellant flow control are also similar to the ones used by the torch igniter.

Similar to the main engine, the RCS must be assembled to the vehicle in a modular configuration where each module will consist of two Pencil thrusters facing in opposite directions. The module must also include the valves and instrumentation required for the operation of the engines. As for instrumentation, each RCE must have a pressure transducer measuring the chamber pressure. This chamber pressure measurement will be used to approximate the thrust being generated by the engine and therefore the impulse created with each firing during flight.

### 2.4.4 Propellant Feed System

The purpose of the propellant feed system is to hold the propellants and provide them to the different systems at the conditions that they require. This subsystem will change slightly between each of Janus' prototypes as different instrumentation is required on each.

It was determined that the propulsion system must operate under regulated pressure conditions. As shown in Figure 20, The feed system will consist primarily of both $LO_2$ and $LCH_4$

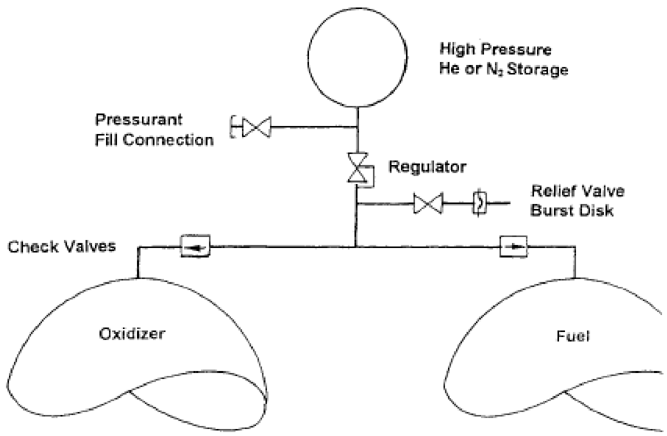


**Figure 18: Simplified bipropellant pressurization system [18].**

propellant tanks and a $GN_2$ pressurant tank. A regulator will maintain the propellant tanks at a constant pressure and lines will be fed from the propellant tanks in order to provide propellant to the separate propulsion systems. This system must also provide measurements of the amount of propellant left in the tanks as well as the quality of the propellants as they are fed into the propulsion systems.

As mentioned above, the propellant feed system will not be incorporated as a separate module but rather it will take part of various modules simultaneously. However, it was decided that each of the tanks will be assigned a separate module in order to facilitate the assembly of the vehicle at its different prototype configurations.

### 2.4.5 Structure

The structure will allow for all the different modules and subsystems in the vehicle to be mechanically integrated with one another. Rigid supports must be incorporated into the structure

for all the components. Also, the structure subsystem will be responsible of providing thrust measurement capability for the main engine during the J-1 test campaign.

It was determined that the structure will carry all the loads that the vehicle will experience. Therefore, no components from other subsystems such as the tanks will bear any loads. The structure must also be built using standard structural beams and tubing.

The overall shape of the vehicle will be defined by the structure and this plays an integral role in the control mechanisms used by the GNC. Different vehicle configurations were visited, as it will be discussed later in this text, and each showed unique structural and dynamic characteristics.

### 2.4.6 Guidance Navigation and Control (GNC)

The purpose of the GNC system is to provide the vehicle with a control algorithm that will allow it to perform the required flight profile. A dedicated team was established for design the GNC system for this vehicle. Unfortunately, their efforts have been focused on another project of the cSETR for the time being. This is not an immediate issue given that the design of the J-1 prototype will not require a GNC system; however, it is imperative to maintain the difficulties associated with the control system in mind during the design process of the vehicle. For example, during the layout design of the vehicle as it will be explained later in this text, the expected difficulty for the control of the vehicle was taken into consideration.

# Chapter 3: J-1 Development

## 3.1 TECHNOLOGY RESEARCH AND INNOVATION ACCELERATION PARK (TRIAC)

The development of some larger scale projects such as the Janus vehicle among others, required an expansion of the current laboratory work capabilities at the cSETR. For this, UTEP has made a partnership with the county of El Paso to lease a plot of land next to an airport in Fabens, Texas. This land will be used to build the new testing facility tRIAc.

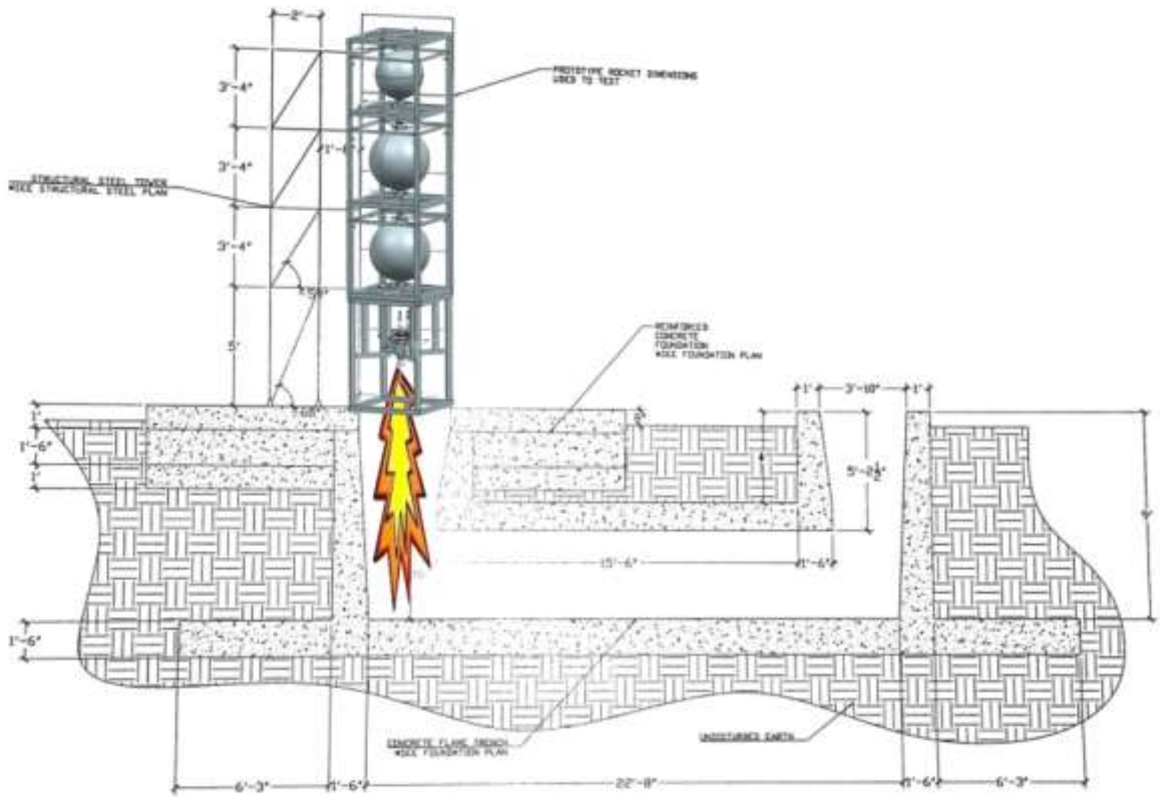

**Figure 19: Alpha site flame-trench configuration with J-1 concept on top.**

Initially, the tRIAc facility will consist of two sites: Alpha and Beta. It will be on the Alpha site where the testing for Janus and Daedalus will take place. The first prototype of Janus, J-1 will be done on a static test stand. For this, it has been devised that a flame trench is to be built in order to deflect the exhaust gases produced by the engine away from any sensitive hardware. On top of the flame trench there is to be a flexible interface that will be able to accommodate different structures that may be used as a rocket engine test stand. Also, at the side of this interface will

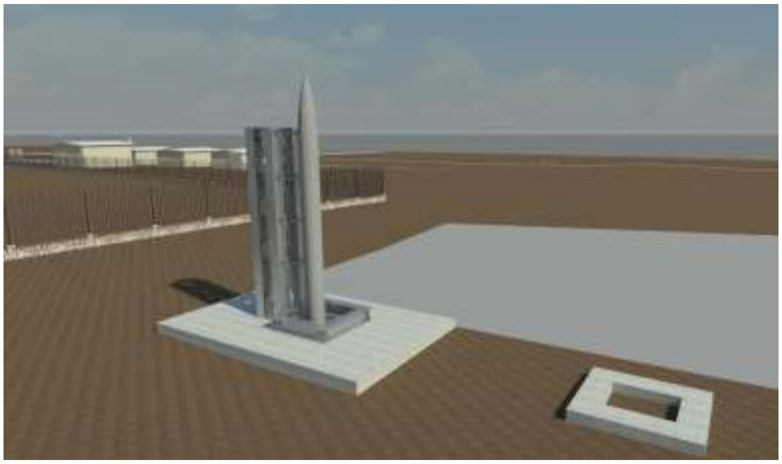

Figure 20: Artist rendering of the Alpha site with a model of Daedalus in place.

stand a structural tower which may be used for additional support for the structures of the test stand or vehicle prototype. Figure 21 shows a rendering of a J-1b concept on top of an architectural drawing of the planned Alpha site test stand and Figure 22 shows a 3D rendering of the tRIAc Alpha site with a model of Daedalus standing on the flame trench.

The interface from the flame trench to the vehicle or test stand will consist of four I-beams arranged in a square around the entrance hole to the flame trench. As is evident on Figure 23, which shows a CAD model of this interface, the I-beams will have a series of bolt holes which will be used to attach the vehicle's structures.

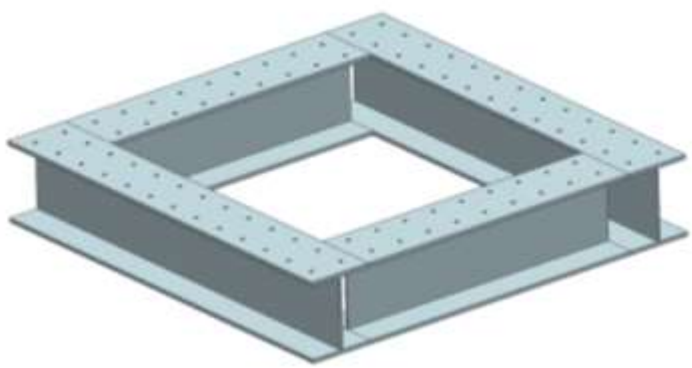

**Figure 21: Alpha site flame trench to vehicle interface.**

To provide for the propellants and different fluids necessary for the operation of the test stand, a fuel farm will be installed. The fuel farm will consist of large cryogenic storage tanks where the $LO_2$ and LNG (LNG will be used in the place of $LCH_4$) will be stored. The fuel farm will be accessible by tanker trucks in order to refill the storage tanks whenever it is needed. To

transport the propellants to the test site, however, a separate transport tank is required. The transport tank must be able to maintain the propellants at cryogenic conditions for long periods of time and so a double walled vacuum-insulated tank is preferred such as the LNG Microfueler shown in Figure 24. This tank will be filled at the fuel farm and later transported to the Alpha site by using a fork lift. There, it will be used to fill the test tanks or the vehicle tanks. A different transport tank will be utilized for both of the LNG and $LO_2$ propellants but they shall have similar characteristics.

**Figure 22: LNG Microfueler.**

The $GN_2$ that will be utilized for purging the tested system as well as pressurizing the test stand and vehicle will be provided through 6K-Type Nitrogen bottles which come pressurized to 6,000 psi. Whenever one of these bottles is empty, it can easily be swapped for a new full bottle by the provider. As it will be discussed in the propellant delivery system progress, this system may also be utilized to maintain a regulated pressure in the test tanks for the J-1 prototype. On that case, a cluster of $GN_2$ bottles will need to be used simultaneously in order to provide the required volume and flow rate of $GN_2$.

### 3.2 Subsystem Progress

The development of Janus has focused on the J-1 prototype. Although all subsystems have seen progress simultaneously, priority has been given to the systems that will take part on the J-1a test stand. Therefore, the center of attention has been given to the development of the test stand structure, the propellant feed system and the main engine subsystem.

Given that a high-level architecture has been set in place for the Alpha site of tRIAc, the structure required for the 2,000 lbf engine test stand has been devised to be built on top of it. Also, the propellant tanks for the test stand have been sized and are currently undergoing procurement. The main engine module, on the other hand, has gone through packaging design and some of its

components have been selected and acquired and are currently being submitted trough acceptance tests.

### 3.2.1 Structures

The structure that will be used during the J-1b tests must closely resemble that which will be used for the flight vehicle on the J-2 and J-3 prototypes. For this, the overall configuration of the vehicle must be approximated. There are many ways that a robotic lander can be configured for flight. In the case of Janus, several concepts were approached and a tradeoff analysis was made between them in order to select the configuration which would be used by the robotic lander. The envelope size of the structure is very closely related to the propellant tanks since they occupy the highest volume of all the subsystems in the vehicle. Therefore, the different concepts consist mainly on different layouts of both the propellant tanks and the $GN_2$ pressurant tank.

From the beginning of the project, the transfer of hardware from the NASA Morpheus project was a possibility. One example was the possibility to utilize some of the propellant tanks that were built for Morpheus yet were never integrated into a vehicle. These tanks were spherical Aluminum tanks with a 48 in outer diameter. Some of the vehicle layouts considered the use of these tanks and the structure was based around them. These layouts came with the great benefit that the cost of development and procurement of the propellant tanks would be eliminated completely. However, these tanks are grossly oversized for the required mission and there is the possibility that they could be too heavy for the CROME-X engine.

Another possibility was one on which the propellant tanks would be sized strictly to the volume required by the mission flight-profile. These customized tanks would limit the flight duration to that for which they were designed and would not allow more ambitious flights to be carried on in the future. However, the use of custom-sized tanks would require a much lighter vehicle and therefore smaller amounts of propellants for each test effectively decreasing the costs associated with every test. The use of customized tanks also allows their geometry to be versatile

and not be limited to a spherical shape of the Morpheus tanks. Several concepts were visited that would use different shapes of custom-sized tanks.

From the different structure layouts that were considered, three were selected to do a trade study. They were called the Snowman, the Spider, and the Mini-Morpheus:

The Snowman consisted of stacking the tanks and the propulsion system vertically one on top of the other as shown in Figure 25. Under this configuration, the CROME-X main engine module would be placed at the bottom of the vehicle, on top of it would be a gap allowing the GNC module to be stacked. On top of the GNC module the different tank modules could be stacked up. The order of the different tank modules could be modified. Given that each tank module will have a different mass, the order on which they are stacked can be changed in order to move the position of the center of mass (CoM) of the vehicle. The CoM position is of great importance to the calculations made by the GNC system and this gives some flexibility as to where it will be. As shown in Figure 24, this configuration can be made with either the Morpheus tanks or custom-sized tanks.

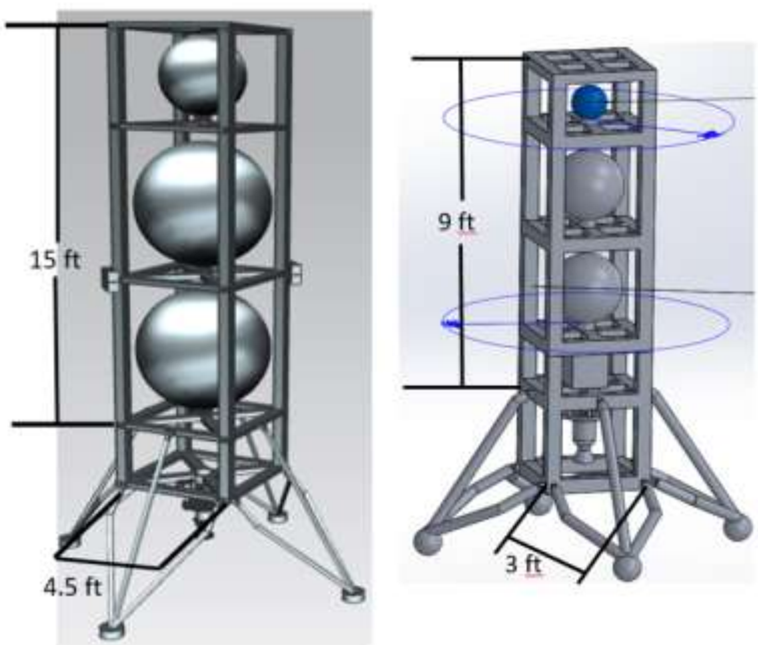


**Figure 23: Snowman configuration using Morpheus tanks (left) and using custom-sized tanks (right) [17].**

The Spider configuration consisted in stacking the propellant and pressurant tanks in a pyramidal shape. Under this configuration there would be two equal size $LCH_4$ propellant tanks placed on either side of a single $LO_2$ tank. On top of the three tanks would sit the $GN_2$ pressurant tank. This design would not permit the use of Morpheus tanks since three propellant tanks would be required and the $LO_2$ tank would be larger than the $LCH_4$ tank. However, several shapes of customized tanks could be considered. Figure 26 depicts a rendering of the Spider configuration

using different shape of tanks. The Spider configuration had the benefit of being compact and easy to assemble; however, this setup creates unsymmetrical pitch and yaw moments of inertia which makes the control of the vehicle more challenging.

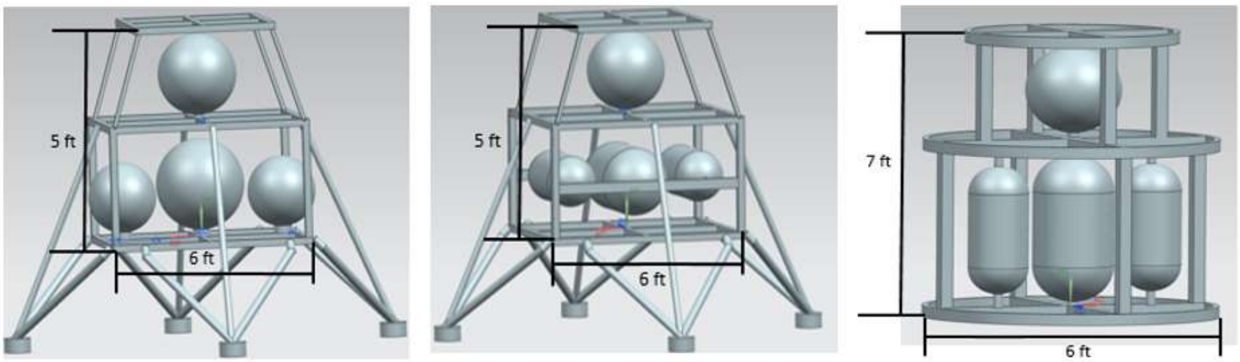


**Figure 24: Spider concept using spherical tanks (left), horizontal cylindrical tanks (center) and vertical cylindrical tanks (right) [17].**

The last configuration studied was the Mini-Morpheus configuration. This layout consisted of having four equal-sized propellant tanks (two $LCH_4$ and two $LO_2$) arranged around a pressurant tank. The propellant tanks would be arranged in a checkerboard pattern having the tanks containing the same propellants be diagonally across from each other.

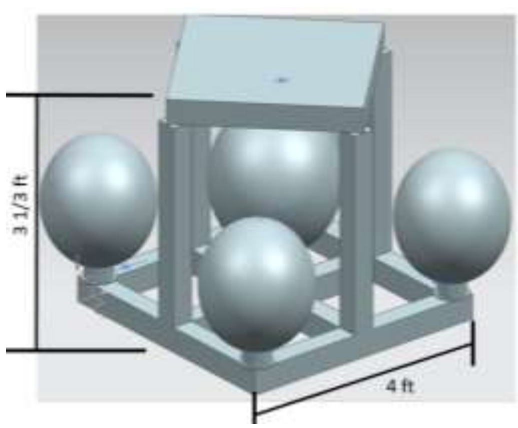


**Figure 25: Mini-Morpheus configuration [17].**

This configuration mimics the design that was utilized by the NASA Morpheus vehicle and hence the name Mini-Morpheus. This configuration also allows a compact design without the issue of unsymmetrical moments of inertia; however, this configuration would require the incorporation of five tanks simultaneously. Tanks proved have shown to be one of the most expensive components in the vehicle and therefore incorporating so many would increase the overall cost of the vehicle.

Form these configurations, a trade-off analysis was conducted in order to select one to pursue. The main aspects which were taken into consideration for the trade-off analysis were the

the overall weight of the vehicle, the maneuverability and the expected cost of the system. These parameters were tabulated into a decision matrix to select the most convenient configuration.

**Table 1: Janus components weight budget.**

| COMPONENT | WEIGHT (lbf) |
|---|---|
| Power (SOFC or batteries) | 50 |
| GNC | 50 |
| Main Engine | 200 |
| RCS | 120 |
| Landing Gear | 150 |
| **TOTAL** | **570** |

The weight associated with each concept needed to be estimated in order make a better comparison between them in the decision matrix. To do this, firstly, some of the components which have unknown weights and that would be used by any configuration were allocated a weight budget as shown in Table 1. This weight was either based on existing hardware or estimated based on similar components made in the past by NASA and others. Afterwards, an estimation of the size of the propellant and pressurant tanks required to complete the mission was done for each configuration. To calculate the weight of these tanks it was assumed that they would be made out of Aluminum 6061 which has a density of 0.096 lbm/in$^3$. For the propellant tanks, a thickness of 0.25" was assigned and for the pressurant tanks the thickness was calculated based on its volume and pressure allowing a factor of safety (FS) of 2 to yield. Once the geometry of the tanks had been estimated, the weight of them was calculated and added to the dry mass of the vehicle. This had to be done in an iterative way since any change in the dry mass of the vehicle affects the amount of propellant required to complete the flight-profile which in turn affects the size and pressure of the propellant and pressurant tanks yielding a different dry mass. However, after a few iterations it was possible to converge into an estimated tank weight.

Finally, the weight of the structure was estimated by calculating the optimal dimensions of the structural beams or tubing to be used. In order to do this, a finite element analysis (FEA) was done for the different configurations. The models were generated using Hypermesh with the Optistruct solver. As shown in Figure 28, the structures were meshed using CBAR elements for

the beams and shell elements for the tank walls. The material properties assigned to all the elements on the different configurations were those of Aluminum 6061. This model was ran using the following load cases:

- Modal analysis.
- Static and dynamic loads from the propulsion systems.
- 5g lateral load.
- 20g landing load.

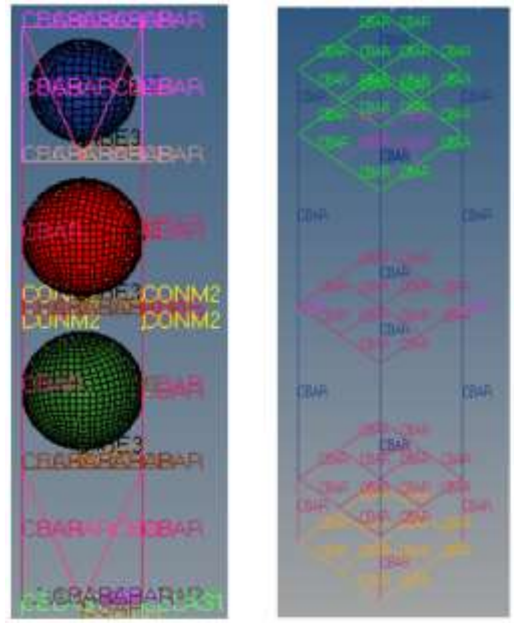

**Figure 26: Mesh of the Snowman concept using Hypermesh [17].**

The cross-section on the CBAR elements was varied in such a way that the structural beams would be optimized for weight while achieving a FS of 2 under all the load cases. Once the dimensions of the beams had been set, it became possible to calculate the weight associated with the structure of each configuration. However, the calculated structure weight was very similar for all the different concepts and was rounded to 300 lb for the ones using custom tanks and 600 lb for the ones using Morpheus tanks. With this information, it became possible to quantify the estimated weight of each concept. Table 2 shows a summary of the total estimated weight for each concept.

With this approximation, it was found that the estimated wet weight of the snowman concept utilizing Morpheus tanks is very close to the maximum thrust output of the main engine. This is undesirable given that the vehicle wouldn't be able to lift-off at the desired acceleration. However, a big portion of the weight for this configuration comes from the pressurant tank. Given that the Morpheus tanks are oversized, it would be possible to operate the system as a blowdown. That is, without the use of a regulated pressurant on board. It was estimated that operating as a blowdown system would decrease the wet mass of this configuration from 2027 lb to 1753 lb. The downside of operating under blowdown conditions is that the supply pressure would inevitably decrease as the propellant system is firing. In the case of the Morpheus tanks, the supply pressure

would decrease by approximately 17% (Calculated using ideal gas law). However, it is possible that the main engine could still operate nominally by adjusting through the throttleable valves. This can be determined through testing during the J-1a configuration. If in the future, a transfer of the Morpheus tanks becomes certain, this option should be considered.

**Table 2: Summary of estimated Janus concept weights.**

| | **Components [lb]** (See Table 1) | **Tanks [lb]** (Pressurant & propellant) | **Fluids [lb]** (Perssurant & propellant) | **Structure [lb]** | **Dry weight [lb]** | **Wet weight [lb]** |
|---|---|---|---|---|---|---|
| **Snowman: Morpheus tanks** | 570 | 433 | 425 | 600 | 1602 | **2027** |
| **Snowman: Custom tanks** | 570 | 246 | 248 | 300 | 1116 | **1364** |
| **Spider: Spherical tanks** | 570 | 248 | 244 | 300 | 1118 | **1362** |
| **Mini-Morpheus** | 570 | 259 | 246 | 300 | 1130 | **1377** |

Once an estimation of the concepts weight had been done, the decision matrix was populated as shown in Table 3. The parameters considered were given a score between 0 and 3 for each concept.

The grades assigned for cost parameter were determined mainly by the number of tanks required for each concept. Thus, the Snowman concept was given the highest score since it only requires 2 tanks to be bought; also, in the case of using Morpheus tanks, the cost of the vehicle would significantly decrease given that the tanks would come at no cost. The Mini-Morpheus and Spider concepts were graded equally in this regard given that, although the Mini-Morpheus requires 4 propellant tanks and the Spider only 3, the tanks for the Spider concept have different dimensions likely increasing the manufacturing cost.

**Table 3: Decision-matrix for Janus concept.**

| | Weight | Maneuverability | Cost | Total |
|---|---|---|---|---|
| **Snowman: Morpheus tanks** | 0 | 3 | 3 | 6 |
| **Snowman: Custom tanks** | 3 | 3 | 2 | 8 |
| **Spider: Spherical tanks** | 3 | 1 | 0 | 4 |
| **Mini-Morpheus** | 3 | 2 | 0 | 5 |

For maneuverability, the grade was based on the length of the moment arm from the engine gimbal to the vehicle center of mass (CoM). The Snowman concepts were given the highest score because, being on a vertical configuration, they allow a longer moment arm. A longer moment arm is beneficial as it allows greater control of the pitch and yaw motions of the vehicle with a smaller angular deflection of the main engine gimbal. On the other hand, the lowest grade was given to the Spider concept. As mentioned earlier, the Spider concept would have unsymmetrical pitch and yaw moments of inertia. Because of this, the gimbal would have significantly different effects when deflecting to one direction or another making it more difficult to control.

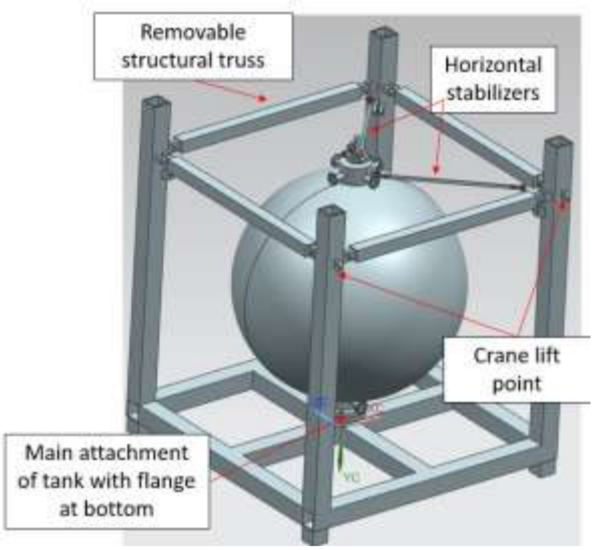

**Figure 27: Tank module model.**

Once the decision matrix had been completed, the focus was shifted towards the design of the structures required by the J-1a and later J-1b prototypes. The modular design approach for these prototypes meant that a structure had to be designed for each module and that the modules must come together in an assembly.

The vehicle tanks, as it will be discussed in the propellant feed system progress, were designed in close resemblance to the Morpheus tanks. These tanks have attachment points at the bottom and top bosses. The top boss has clevis joints to attach horizontal rods from the tank to the structure while the bottom boss has a flange which would also attach the tank to the structure using bolts. Based on these interfaces, the structure for the module was designed around the spherical tanks. As shown in Figure 29, the structure of the tank module consists mainly of welded square structural tubing. However, in order to facilitate the assembly of the module and add or remove the tank, removable trusses were incorporated at the top of the structure. Also, in order to allow the vertical stack-up required for the J-1b prototype, attachment points were added to enable a crane to lift the module when necessary. Two identical modules will accommodate the propellant tanks while a slightly smaller one will be used for the pressurant tank. Figure 30 shows the way that the tank modules would be assembled one on top of the other.

**Figure 28: Vertical assembly of tank modules.**

The J-1 prototype will perform as a static testbed. For this, a stationary structure on which to attach the vehicle was designed. Given that the Daedalus program is being developed under a very similar timeline to Janus, the same structure will be used for the testing campaign of both the CROME and the CROME-X engines. For this reason, the structure was designed as a modular system; that way the components could easily be switched as the testing of each engine requires.

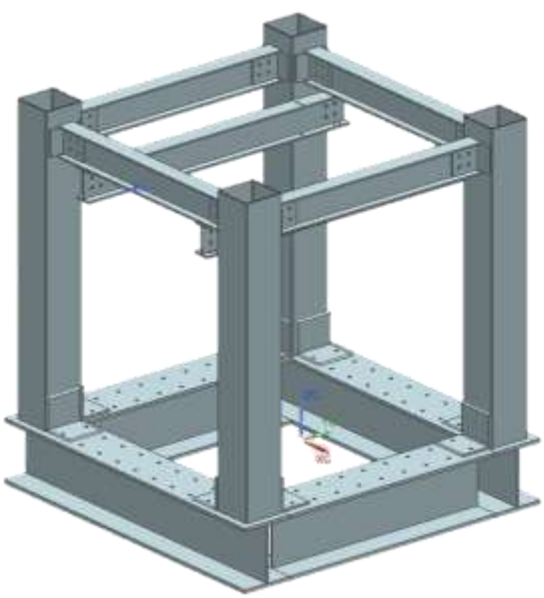

**Figure 29: Static J-1 structure.**

An interface was defined by the design of the tRIAc Alpha site as four I-beams to which the J-1 static structure will to attach. A semi-

permanent structure will be built atop this interface using standard structural beams. As shown in Figure 31, four columns will be attached at each corner of the flame-trench interface from the Alpha site and then connected at the top with I-beams. This creates an elevated platform onto which the rocket engines can be attached. This design effectively carries first the weight of the engine and later the thrust loads.

One of the main goals of the J-1a prototype is to test the performance of the CROME-X engine. In order to do this, a method of measuring thrust must be available. However, when moving towards the J-1b configuration, thrust measurement will no longer be necessary nor desirable because the prototype will be assembled as the flight vehicle will be. Because of this, a load cell module (LCM) will be implemented which can easily be attached and removed from the static structure.

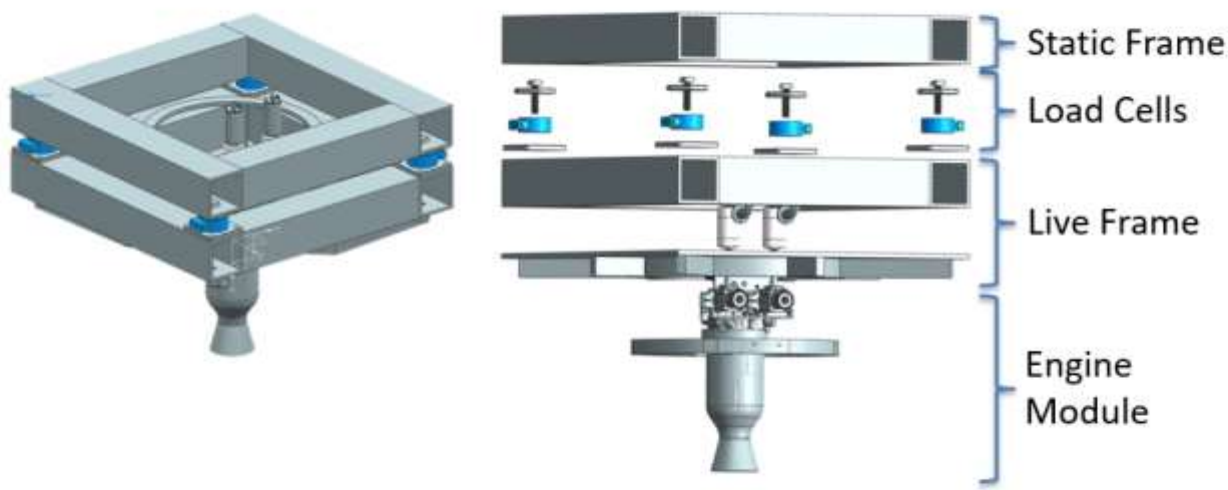


**Figure 30: Load cell module (LCM) assembly (left), exploded view (right).**

The LCM is composed of four low profile tension and compression load cells [17] which will be placed in between two frames. Each frame will be made from welded structural tubing. The top frame, called the static frame, will be firmly attached to the static structure while the bottom frame, called the live frame, will be attached to the engine module. The thrust from the engine will be transferred to the live frame and compress the four load cells. The LCM assembly allows the load cells to be changed depending on the expected thrust output from the engine that

will be tested. Since load cells have an accuracy rating based on a percentage of its maximum capacity, it is recommended that a load cell with a load capacity similar to the expected load to be applied is used. Thus, different load cells would be used between the CROME and CROME-X engines. Having four load cells not only allows for thrust measurements, it also makes it possible to calculate the position of the thrust vector during the engine fire and find any misalignment or fluctuations in it.

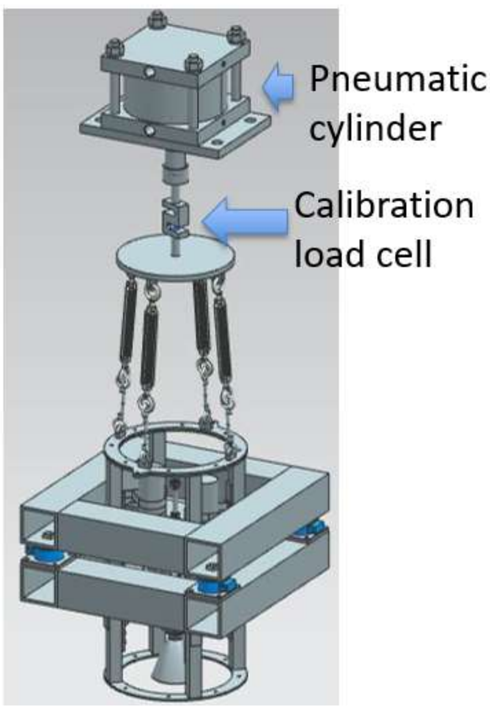

**Figure 31: LCM calibration system with CROME module installed.**

In order to gain accurate thrust data, the LCM must be calibrated prior to each test. The stiffness of the system changes as the propellant lines leading to the main engine get chilled to cryogenic temperatures and then pressurized to their operating temperature. Since no personnel will be allowed at the Alpha site once the system has been pressurized, the calibration process must be done remotely. Following the mentorship from JSC engineers, it was decided that the calibration would be done by using a pneumatic cylinder in a similar design to the one used at Test Stand 401 at WSTF during tests of the RS-18 $LO_2$-$LCH_4$ tests. The calibration system will be operated as follows: Once all tubing and instrumentation has been chilled, the tare value of the load cells will be zeroed out in order to account for the dead weight of the system. Then, a known load will be incrementally applied through the pneumatic cylinder based on the bore area and the pressure applied. This force will be increased up to the maximum expected load that will be applied by the engine. By assuming that the load will be equally distributed among the four load cells in the LCM, data from the voltage output compared to the force applied can be generated. Once the calibration data has been collected, the pneumatic cylinder can be depressurized and the hot-fire test can be completed.

Once the J-1a testing campaign has been completed, the LCM and the calibration system will be removed from the static structure in preparation for the J-1b prototype. With the LCM and calibration system out of the way, it will be possible to stack the tank modules on top of the static structure as it would be done for the flight vehicle allowing to test the integrated propulsion systems and the propellant feed system.

An FEA was done on each individual component of the J-1 stationary structure and LCM which confirmed the soundness of it. Factors of safety of well above 5 were calculated during this analysis. However, the stiffness is required to be as high as possible (>500 Hz) in order to avoid interfering with the thrust measurements and modal analysis of this structure showed unsatisfactory natural frequencies. Therefore, some modifications might be necessary for the design.

**3.2.2 Propellant Feed System**

Focus for the propellant feed system design has mainly been set on sizing and acquiring the test propellant tanks as well as the pressurization system. Also, a preliminary piping and instrumentation diagram (P&ID) has been drawn in order to identify the required instrumentation that will be necessary for the J-1 tests.

In order to obtain an approximate weight for the different Janus concepts considered, sizing of the propellant tanks was done for each one individually. This had to be done through iterations in order to get an accurate estimate of the total vehicle weight. For this, an Excel spreadsheet and MATLAB script were generated in order to accelerate the calculations. The sizing of the propellant tanks was done as follows:

1. Based on the theoretical performance of the main engine ($I_{sp}$ vs thrust), the total amount of propellant required for the mission profile was calculated.
2. A 50% margin is added to the amount calculated above. This is added as a factor of safety in case the main engine has a lower performance than predicted. Also, some propellant will be burned to perform flight corrections which have not been accounted for in step 1.

3. The propellant which would fill the propellant lines as well as the propellant which would be left unused in the tank after the flight is done, must also be accommodated. For this, an estimation of the interior volume in the propellant lines was calculated and added to the total amount. This was approximated to 15 lbm of both $LO_2$ and $LCH_4$. Also, a 3% of the volume was assumed to stay unused in the tank and was added to the total amount of propellant required.
4. After the test tanks are filled with propellants and final test preparations are done, some of the propellant will inevitably vaporize. 20% of the total propellant was assumed to be lost to boil-off and was added to the total approximation.
5. Based on the total amount of propellant calculated and assuming a spherical shape, an internal radius for the tank was calculated. This radius was then rounded up to the nearest ½" in order to accommodate some ullage volume as well as potentially make it easier to manufacture or find commercial off-the-shelf (COTS) tanks.

The ratio of densities (ρ) between $LO_2$ and $LCH_4$ (i.e. $\frac{\rho_{LO_2}}{\rho_{LCH_4}}$) is approximately 2.7. That means that in order to have the same volumes for each tank, the mixture ratio (which is based on mass) must be 2.7. However, as it will be explained in the CROME-X section, because of the addition of film cooling, the MR for this system is 1.89. Thus, the $LCH_4$ propellant requires a larger volume than the $LO_2$. In the future, however, the FFC on the main engine will be replaced by a regeneratively cooled chamber and the MR will then be 2.7. The propellant tanks in J-1 will therefore be made the same volume for $LO_2$ and $LCH_4$ in order to better resemble the conditions that will be flown in the future and also bring the cost of manufacturing of the tanks down. The calculated size of the $LCH_4$ tanks was therefore the one used for the final weight estimation of both $LO_2$ and $LCH_4$ tanks for the concept tradeoff analysis.

Focus was shifted towards the design of the J-1 test setup once the trade-off analysis had been completed. A test plan for the CROME-X engine was written to determine what would be required for each test and it was found that the most demanding test would be a 40 second burn at full thrust (2,000 lbf). This test would require more propellant than the actual flight would; that is

because during the flight, the main engine will not be firing at full thrust and it will throttle down with time.

**Table 4: J-1 tanks characteristics.**

| | $LO_2$ | $LCH_4$ |
|---|---|---|
| Propellant required for test[1] | 40 gal. | 58 gal. |
| Propellant required at fill-up[2] | 49 gal. | 70 gal. |
| Minimum tank ID required | 27.8” | 31.3” |
| Actual tank ID | 32” | 32” |
| Actual tank inner volume | 74.3 gal. | 74.3 gal. |
| Ullage percentage at fill-up | 34% | 6% |

[1]Volume of propellant required for a 40s burn at full-thrust with a 50% margin, unused propellant in tank and propellant in feed lines.
[2]Extra 20% margin added to accommodate boil-off.

The J-1 tanks were sized according to the requirements of the main engine test campaign. Although an analysis was made that showed it is feasible to fly a vehicle with the tanks sized for J-1, it was decided that non-flight tanks would first be procured. Therefore, sturdy and heavy steel tanks will be used for the static tests and later, flight-ready tanks will be optimized for the J-2 and J-3 prototypes. The same margins listed above were used for sizing the J-1 prototype tanks yielding a tank inner diameter of 32 inches as is summarized in Table 4.

A preliminary design for these tanks was made based on the design made by Morpheus. A CAD drawing was provided by the JSC team and a few modifications were made to it in order to fit the requirements of the J-1 prototype. The propellant tank will be made from two hemispheres welded together. On each hemisphere, a boss will also be welded which will have the inlet and outlet ports as well as the mechanical attachment points for the tanks. As seen in Figure 34, the bottom boss will have a flange which will be bolted to the structure and the top boss will have attachment points for horizontal support trusses. The top boss will also have the inlet fittings for the pressurizing gas while the bottom boss will have the liquid interface fittings for the filling and draining of the liquid propellants. As of now, all fittings are to be Quick-Clamp sanitary fittings for 1.5” OD tubing on the liquid interfaces (bottom boss) and standard AN 37° flare fittings for the gaseous interfaces (top boss). The tanks will be fitted with capacitance-based liquid level sensors as well as thermocouple probes at different heights within the tank in order to measure the amount of propellant in the tank. Another possible method

to do this that could effortlessly be implemented is the use of a delta-pressure transducer in order to measure the difference in pressure between the gas at the top and the liquid at the bottom of the

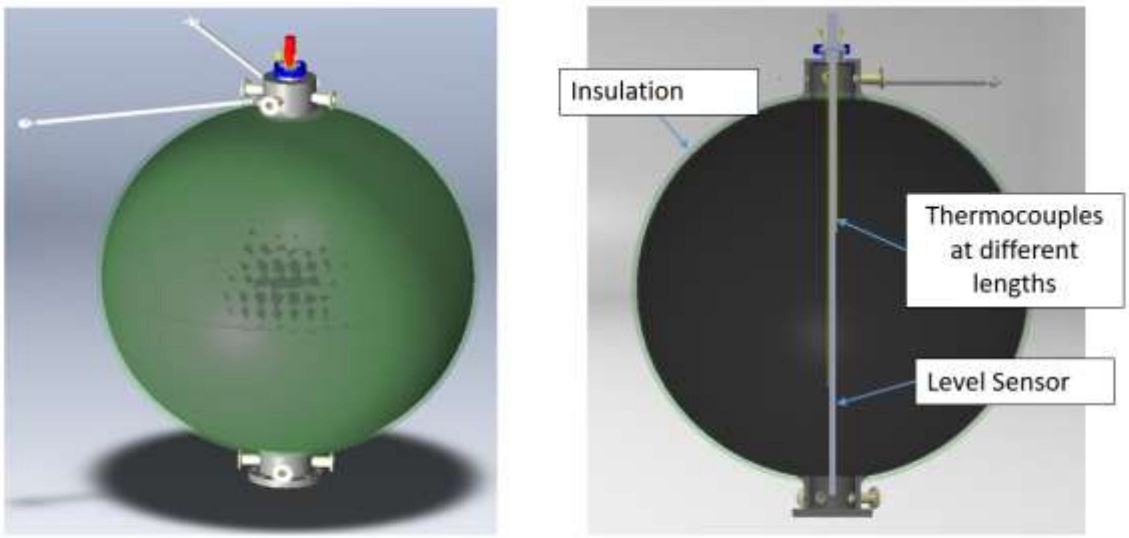


**Figure 32: Propellant tank CAD. Isometric view (left). Cross sectional view (right).**

tank. From this measurement, the height of the propellant within the tank can be calculated.

To keep procurement costs down, it was decided that, similar to Morpheus, these tanks would be single-walled and wrapped in insulation. Cryo-gel is often used by the industry and has been successfully used by the cSETR in various projects. Given its high thermal resistance value and accessibility, it will be used to wrap the propellant tanks as well as all the propellant lines leading out of them.

A piping and instrumentation diagram (P&ID) was drawn in order to identify the instrumentation and hardware required to operate the J-1 prototype. Also, this P&ID will be used as a reference to write the required testing procedures.

With the P&ID in place, it became possible to size the feed lines going from the propellant tanks to the main engine as well as determine the required nominal tank pressure. Based on the required instrumentation and hardware between the tanks and the main engine, an estimation of

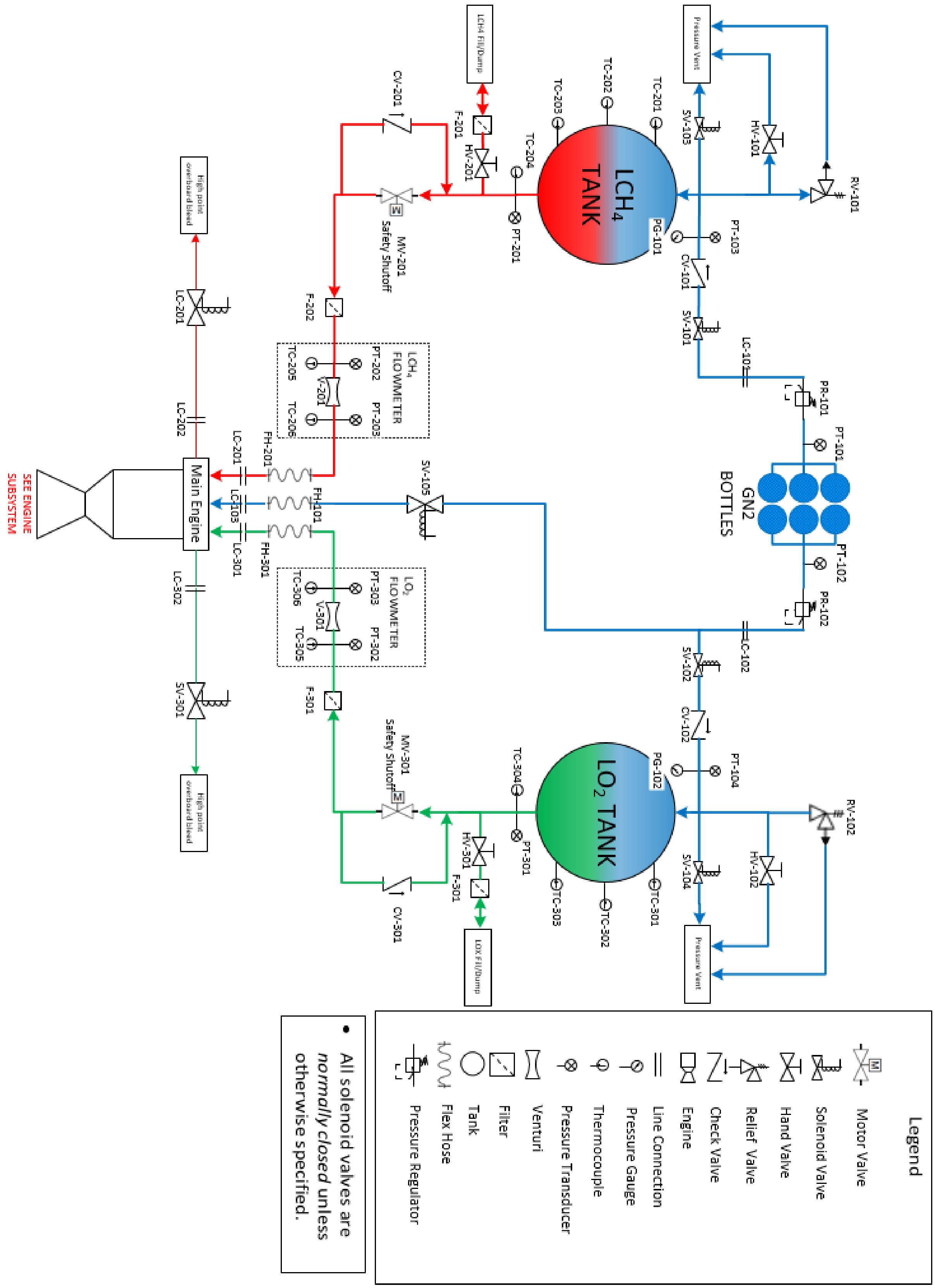


Figure 33: J-1 P&ID

the pressure losses was done. The CROME-X has different flow and pressure requirements for the propellants at different thrust levels yet the most demanding conditions occur at its maximum thrust. Therefore, that was used as the reference to size the lines. As seen in Figure 35, the only hardware in this section is a motorized shut-off valve, a filter and a Venturi flow meter. Using minor loss coefficients found in the Fluid Mechanics textbook by Çengel and Cimbala [18], as well as hardware specifications by the hardware suppliers, an estimation was made for the major and minor pressure losses in the system.

**Table 5: J-1 pressure loss summary.**

| Hardware | Pressure Loss: $LO_2$ | Pressure Loss: $LCH_4$ | Comment |
|---|---|---|---|
| Major Loss | 0.6 psid | 0.6 psid | Assumed 10 ft. of 1.5" OD stainless steel tubing. |
| Inlet from tank to tube | 0.3 psid | 0.3 psid | $K_L$=0.5 (Sharp-edged pipe inlet) [18]. |
| Filter | 5 psid | 5 psid | Typical pressure loss associated with filters. |
| Shut-off valve | 7.7 psid | 7.1 psid | $C_v$=15 (similar to main engine valve). |
| Venturi flowmeter | 3 psid | 3 psid | Estimated by vendor (FlowMaxx Engineering). |
| Contraction | 0.1 psid | 0.1 psid | Gradual contraction fitting from 1.5" tube to 1" CROME-X main valve. ($K_L$=0.04 [18]). |
| Fittings | 0.7 psid | 0.6 psid | 15x threaded unions $K_L$=0.08 each [18] |
| Bends | 0.7 psid | 0.6 psid | 4x 90° smooth bends $K_L$=0.3 each |
| **TOTAL** | **18.1 psid** | **17.3 psid** | |

The pressure losses were calculated on an Excel spreadsheet such that the tubing diameter could be easily modified to find an acceptable pressure loss. 1.5" OD tubing was found to have a pressure drop of approximately 18 psid on the $LO_2$ line and 17 psid on the $LCH_4$ line at full thrust conditions. Table 5 describes the pressure drop contribution by each piece of hardware in the lines. 37° AN flare fittings or Quick-Clamp sanitary fittings will be used on every hardware interface. The main engine has a minimum inlet pressure of 325 psia; therefore, accounting for the pressure losses on the lines and hardware leading from the propellant tanks to the main engine, a minimum

tank pressure of 343 psia is required. Therefore, a minimum operating pressure of 350 psia was defined when procuring the propellant tanks.

Two options are typically used as pressurant for regulated pressure fed systems: helium or nitrogen. Given that helium has a much lower saturation temperature and density than nitrogen, it was decided that it would be used to pressurize the flight vehicle. However, to reduce development costs, gaseous nitrogen ($GN_2$) will be used during the tests of the J-1 prototypes.

The provider Air Liquide, which will be one of the supplier for fluids at the tRIAc facility, recommended the use of 6K Type cylinders for this application. These cylinders come at a pressure of 6,000 psia and have an internal volume of approximately 1.5 $ft^3$ (11.2 gal.). To estimate how many nitrogen bottles would be required for each test, an analysis was made using the ideal gas law and calling on conservation of mass. As shown in Figure 36, it was assumed that the $GN_2$ must

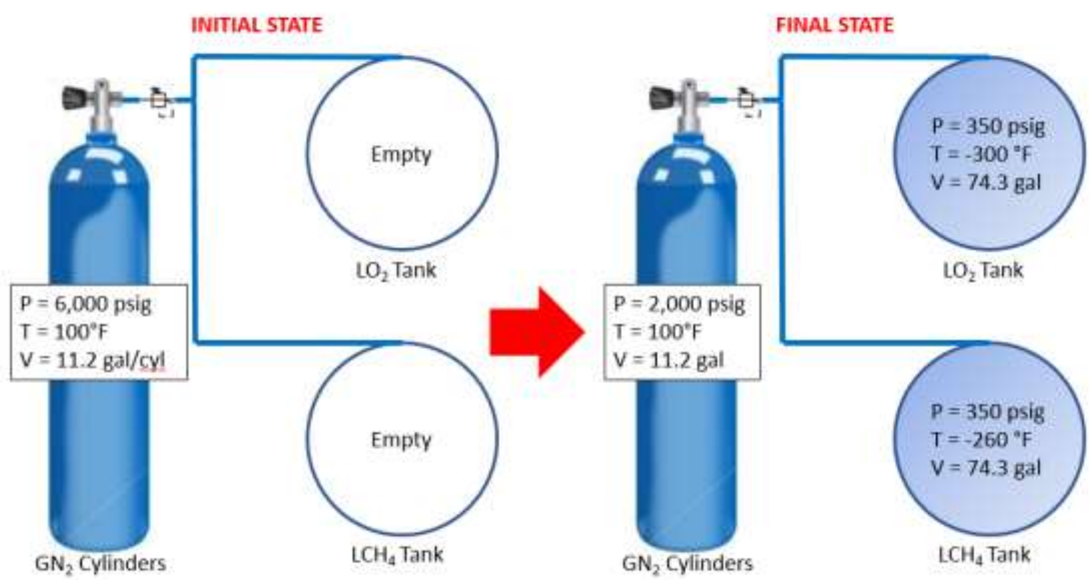


**Figure 34: State assumptions for $GN_2$ requirement estimation.**

completely fill the propellant tanks and that it will cool to the temperature of the cryogenic propellant. Even though in all likelihood this will not be the case, it was assumed like that in order to obtain a conservative estimation. Through this calculation, it was found that four 6K-Type cylinders of $GN_2$ would be needed for each test.

Once this requirement was set, the provider Air Liquide recommended the use of a 6-pack containing six of the 6K-Type 6,000 psi $GN_2$ cylinders. Although it will most likely be more that the required amount, the extra $GN_2$ can be employed for purging purposes before and after each test.

### 3.2.3 CROME-X

The development of the CROME and CROME-X is being done in parallel and most of the progress up to date applies to both engines given their similarity. The difference between the two for the first iteration lies mainly in the maximum thrust output expected. Once the high-level requirements had been set, a theoretical design was made in order to size the different components of the engine as well as define theoretical operational requirements.

Based on NASA's Chemical Equilibrium with Applications (CEA) software, a MATLAB script was written by the CROME-X team that would calculate the theoretical performance of the engine at its different thrust levels. It was decided initially to have a combustion MR of 2.7 which would allow the vehicle tanks to be the same volume. That is why this configuration was used for the CEA analysis mentioned above which yielded an acceptable theoretical efficiency calculation and relatively low combustion temperatures. However, since the first iteration of the engine will use a pintle injector, it became necessary to incorporate fuel film cooling (FFC) which is measured as a percentage of the total $LCH_4$ flow-rate. Based on the experience of the Morpheus main engine, the maximum FFC allowed was limited to 30% yet the optimal amount of FFC flow will be tested for. With FFC at its maximum allowed flow, the total flow results in an MR of 1.89. That MR will be differentiated from the combustion MR by calling it the system MR.

The CEA software provides the characteristics of the combustion products at the defined MR of 2.7 such as the characteristic velocity (C*). Based on this information it became possible to estimate other performance characteristics such as the $I_{sp}$ at several combustion chamber pressures. The maximum chamber pressure which would match the 2,000 lbf output was designed to be 232.8 psia. Afterwards the chamber pressures corresponding to different thrust outputs within

the 500 to 2,000 lbf range were calculated. This in turn made it possible to determine the required propellant flow rates.

In an effort to describe the test campaign of the J-1a prototype, a test plan was written listing the goals and objectives projected for each test. The plan was written in a way that each successive test increased in difficulty and risk. This would allow for each test to be done with confidence based on the data provided by the previous test. Table 6 describes the objectives of each test as planned.

**Table 6: J-1a test plan.**

| No. | Test Name | Description |
|---|---|---|
| 1 | Igniter operation | Fire the igniter by itself to verify its reliability under the J-1 fluid system configuration. |
| 2 | Sweep-through MR | 5 s burns at increasing MR up to the nominal 2.7 allowing to verify ignition over an MR range. Starting fuel-rich results in lower temperature combustion reducing risk of failure. |
| 3 | Increase burn time | Gradually increase burn duration at full thrust and nominal MR until a steady 40 second burn is achieved. |
| 4 | Step throttle | Full duration burns at different power level percentages (PL). |
| 5 | Live throttle | Throttle over the full PL range during a full duration burn at different throttle cycles. |
| 6 | Optimize FFC | Gradually decrease FFC flow to find the lowest amount which still allows a 40 s burn. |
| 7 | Step throttle at optimal FFC | Repeat Test 4 with optimal FFC setting. |
| 8 | Janus flight-profile | Simulate Janus' mission duty cycle (MDC) in the J-1 configuration. |

*Note: Tests 1 – 5 will be done with max FFC flow (30% of total $LCH_4$ flow).*

As mentioned above, this engine will use a pintle injector. Figure 37 shows a cross-section of it on which its evident that the injector was sized to be $LCH_4$-centerd meaning that the $LCH_4$ flow would be incorporated as the radial component of the pintle. The injection orifices were sized based on the required flow rate providing a certain amount of pressure drop (ΔP). In order to prevent chugging

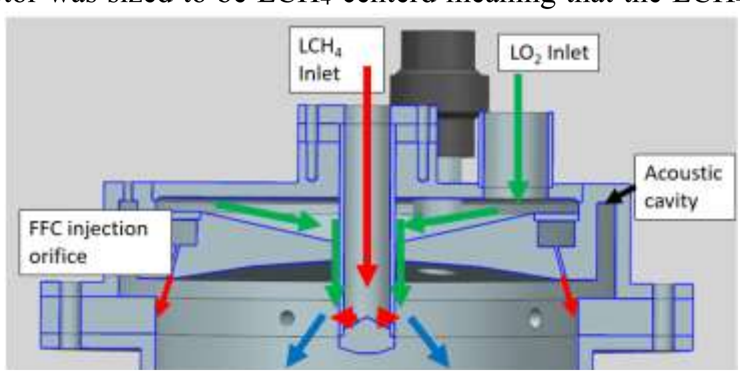

**Figure 35: Injector cross-section view.**

**Table 7: CROME-X operational requirements.**

| Requirement | Value |
|---|---|
| Thrust | 2,000 to 500 lbf |
| MR | Combustion: 2.70<br>System[1]: 1.89 |
| Chamber Pressure ($P_c$) | 233 to 75 psia |
| System $I_{sp}$[1] | 219 to 168 s |
| Inlet $LO_2$ Conditions | Min. Press: 325 psia<br>Temp: -300 to -273 °F |
| Inlet $LCH_4$ Conditions | Min. Press: 325 psia<br>Temp: -260 to -225 °F |

[1]Defined including 30% FFC (max allowed).

instabilities, literature recommends to design the injector orifices to have a $\Delta P$ of at least 20% of $P_c$ [2]. Given the deep throttleability of the CROME-X, maintaining a $\Delta P/P_c$ of 20% at the lowest thrust requires extremely small injection orifices and yields very high $\Delta P$ values at the high end of the thrust. For this reason, the orifices were sized to provide a $\Delta P/P_c$ of only 10% at the low end and yield around 30% when flowing for 2,000 lbf of thrust. Adding the minor and major losses associated with the injector manifolds, results in the propellant inlet conditions at the main valve listed in Table 7.

For the first iteration, the main engine will have several interchangeable parts that will allow to tweak the parameters necessary to follow the test plan. Some of these interchangeable parts include a needle valve which would be used to control the FFC flow, a removable pintle post allowing to modify the injection orifices and interchangeable acoustic cavity blocks used to dampen acoustic instabilities.

***3.2.3.1 Engine Component Selection***

The CROME-X engine will be throttled by using its main valves; therefore, they are a crucial component of the engine. The main engine valves will control the flow of propellants going into the engine through its operating position. Precise valve position control and repeatability are paramount to vary the thrust for vehicle dynamic control [19].

Requirements were set for the valves based on the operating conditions of the engine at its different throttle levels. Several options were reviewed and after considering them, it was decided to use a ball valve given that they require only a quarter turn to be completely opened or closed.

However, regular ball valves give a very nonlinear flow response based on the position of the valve. To resolve this, a type of ball valve with a v-shaped port was considered. This type of valve allows a much more streamlined flow control through the position of the valve.

One of the requirements for the selection of the valve is that a maximum of 5 psid shall be lost in its fully open position. It was found that this corresponded to a flow coefficient ($C_v$) of 15. Various valve suppliers were explored and a 1” valve by Habonim Industrial Valve & Actuators was selected to provide a 60° v-port ball valve which met the control and pressure drop requirements. The supplier provides theoretical data for the corresponding $C_v$ at different valve positions from fully open to fully closed. This data was used to correlate the position of the valve to the expected thrust output from the engine. The valves were bought with 1” tube inlets to which Quick-Clamp sanitary fittings from McMaster-Carr were butt-welded. These types of fittings allow an easy removal of the valves in case that they need servicing.

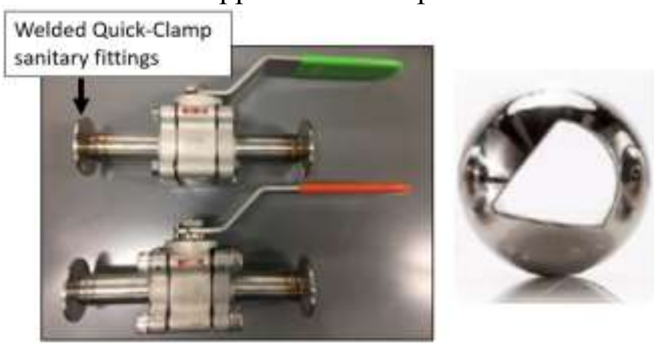

**Figure 36: Habonim ball valves (left). 60° v-port (right).**

An actuator was selected based on the specification of the valves as well as the engine’s control requirements. Therefore, the torque required to open the valve (as specified by the vendor) was set as a requirement for the torque output of the actuator and the valve reaction time from fully closed to fully open was set to a maximum of 0.5 s. Also, another control requirement of the engine specified that at least 256 positions must be available to the control system between fully closed and fully opened.

Based on those requirements a DC motor was selected as the actuator for the valves combined with a 71:1 gear ratio gearbox. At this configuration, the actuator outputs 255 lbf-in of torque at 42 RPM (0.36 s from closed to open) with more than the required 256 steps [19].

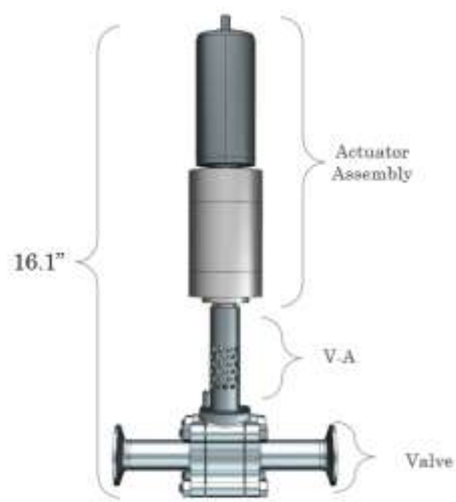

**Figure 37: Main valve assembly.**

However, it was found that the minimum operating temperature for the gearbox is of -22°F and therefore could not be mounted directly on the valve as the flowing cryogen would cool the gearbox below that temperature. An interface named the Valve-Actuator (V-A) connector was designed to act as a thermal standoff and also transfer the required torque from the gearbox to the valve. Computational analysis using Ansys was done during the design process of the V-A in order to ensure that the gearbox temperature would not decrease below the rated value and that the V-A would withstand the stresses associated with the torque of the actuator. The V-A connector was 3D printed at the W.M. Keck Center at UTEP using Titanium Ti-6Al4V given the high strength and low thermal conductivity of this material.

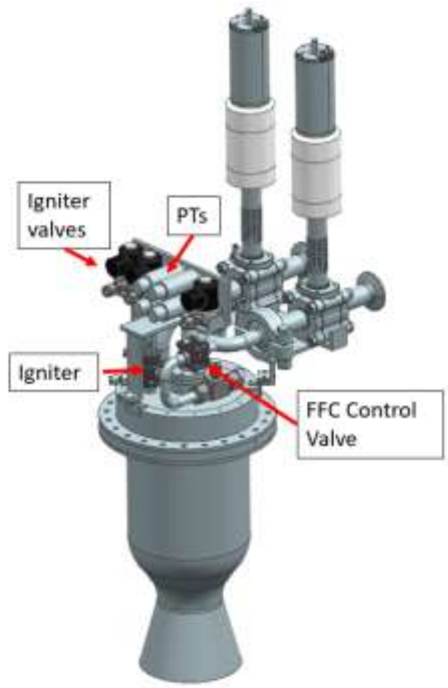


**Figure 38: CROME-X complete assembly.**

Once the main components for the engine were selected, the engine module was modeled so that it would accommodate all its required components within an assembly. Space was allocated for the FFC cooling valve, the igniter and purge valves and all the instrumentation required such as pressure transducers (PT) and thermocouples (TC). A stand was modeled for all these components as well as an attachment point for the main valves. Figure 40 shows the complete assembly of the CROME-X module.

As is evident in Figure 41, some of the components of the CROME-X will be bolted together. At the interfaces that two parts will come together, it is necessary to incorporate a seal. Based on a recommendation from the team's

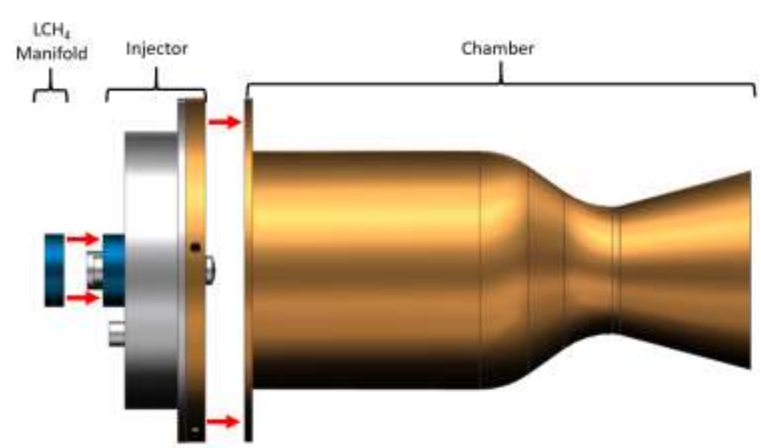


**Figure 39: CROME-X bolted interfaces.**

mentors at JSC, a Teflon ePTFE (expanded Polytetrafluoroethylene) seal called GORE was selected given its expendability and low price. This type of seal is rated for temperatures between -450°F and 600°F and pressures up to 580 psig making it ideal for cryogenic service interfaces like the one between the $LCH_4$ manifold and the injector body. However, it will also be placed in the injector-to-combustion chamber interface which is expected to see temperatures higher than its rated 600°F. Nonetheless, NASA has experience using the same GORE seal on a similar high temperature interfaces successfully and since having a leak on that particular interface is not critical it was deemed appropriate to it on the injector-to-chamber interface.

### *3.2.3.2 Engine Component Tests*

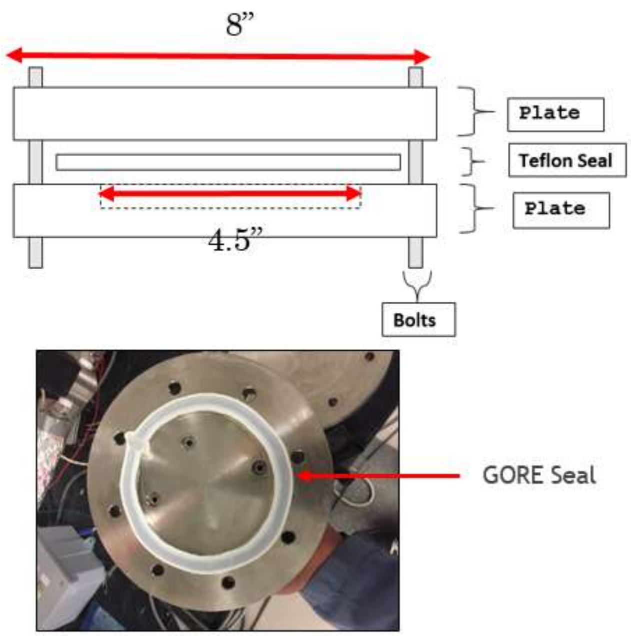


**Figure 40: GORE seal test plates setup [19].**

Tests of the selected components were scheduled to be done in order to qualify their performance under simulated CROME-X operating conditions. The first of these tests was done for the GORE seal. It became apparent that a method to quantify the effect of extreme temperatures on the leak rate and gasket pressure as well as the amount of creep over time was necessary. In order to do this, a pair of plates simulating the flanges of the bolted interfaces were built. One of these plates had a small chamber while the other had an inlet and outlet port as shown in Figure 42. The setup was subjected to temperature cycles by flowing $LN_2$ until the wall temperature reached -200°F and then allowing it to heat up to ambient temperature.

In order to measure the leak rate from the seal, $GN_2$ was pressurized to 200 psia inside the chamber between the two plates. The pressure was held for approximately 10 min. while the temperature and pressure of the gas was recorded. Based on those pressure and temperature

measurements, a value for density of the gas was taken using the Reference Fluid Thermodynamic and Transport Properties Database (REFPROP) tool and, assuming a constant volume, the initial and final gas mass inside the system was calculated. This was done twice for each temperature cycle, both at cryogenic and ambient temperatures and with this method, a leak rate was measured in lbm/s. The leak was also evaluated by submerging the test article in water while it was at ambient temperature and through visual examination, assess whether bubbles are forming in the water.

The minimum gasket pressure recommended by the GORE seal supplier is of 2,000 psi and it was exerted through the preload on the bolts. Each bolt was measured using a micrometer before and after being assembled on the test flanges. The elongation experienced by the bolt after it had been preloaded, was used to calculate the clamp-force that it was applying to the flange. With this information, the bolts would be tightened or loosened such that the total applied clamp-force corresponded to minimum the required gasket pressure. After every temperature cycle (at room temperature) the length of the bolts was measured again in order to calculate the effect that the cryogenic temperature had on the preload. A total of five temperature cycles were done without adjusting the preload on the bolts and the bolt lengths were recorded after each one.

Although further examination of the test data is required to evaluate the error associated with the measurements, it was found that the leak rate of the GORE seal at cryogenic temperatures was in the order of $10^{-6}$ lbm/s. Even though the preload was calculated to have dropped significantly throughout the five cycles, the amount of leak detected remained in the same order of magnitude. Also, no visible leaks were ever observed while the test plate was at cryogenic conditions nor were any visible bubbles formed while the test article was submerged under water and pressurized through the five cryogenic temperature cycles. Therefore, the use of this type of seal was validated for interfaces that will be subject to cryogenic temperature; however, the preload applied should be monitored constantly and maintained at the nominal value after each test. A test to validate the use of the GORE seal at high temperatures (over 600°F) is currently being developed. The same basic setup will be used, however, this time the test article will be heated by either inserting it in a furnace or placing it on top of an electric heater.

Another test that has been scheduled is for the main throttleable valves of the CROME-X. There are three main verifications to be made: The first is a leak check of the valve; cryogenic valves normally are designed with a long stem that prevents some of the internal seals from failing due to low temperature. However, a long stem would result in a very long CROME-X module; and so, it was decided to remove the long stem and operate the valve without it. Leak tests in a similar configuration as they were done to the GORE seals will allow to verify that the valve can indeed be operated without the long stem.

The second test will be done to demonstrate that the V-A thermal standoff performs as expected and does not allow the actuator gearbox to cool to a temperature under -22°F. For this test, $LN_2$ will flow inside the valve at similar conditions that it would experience during hot-fire. Throughout this test, the temperature at the top of the V-A connector (where it would be in contact with the gearbox) will be monitored until a thermal steady state is achieved. The V-A will be accepted if the temperature never drops below -22°F at that location.

The final test of the valves would consist of verifying the calculated flowrate vs valve-position plot. As mentioned before, the valve manufacturer provided $C_v$ vs valve position data which was used to calculate the flowrate corresponding to valve position. This data will be verified by flowing first water and then $LN_2$ through the valve and record the pressure drop through the valve along with the flow rate going through it. If the new data does not match the supplier provided data, the new $C_v$ data will be used for future calculations of the flowrate expected per valve position. These tests will also be used to develop control software that will allow the valves to be set at specific positions during hot-fire.

Once the injector is manufactured, preliminary water-flow acceptance tests will be made. The purpose of these tests is to verify the design calculations made on the injector. A test setup was built in a configuration as is seen in Figure 42. The water reservoir will be filled with distilled water which will be pumped up towards the injector which is mounted on the top of the cage facing down. Turbine flowmeters will be used to measure the total flow of water going into each of the injector inlets which will be controlled by using a globe valve placed downstream of the flowmeter.

By measuring the static pressure on the water flow upstream of the injector, the pressure drop across the injector elements can be found. This is an important parameter given that the injection orifices were designed to a specific pressure drop at certain flowrates to avoid chug instabilities and therefore the theoretical design can be corroborated. Also, by flowing water over a wide range of flowrates through the injector and reading the pressure drop, a discharge coefficient ($C_d$) vs flowrate curve can be created providing better understanding of the flow behavior through the injector at different flowrates.

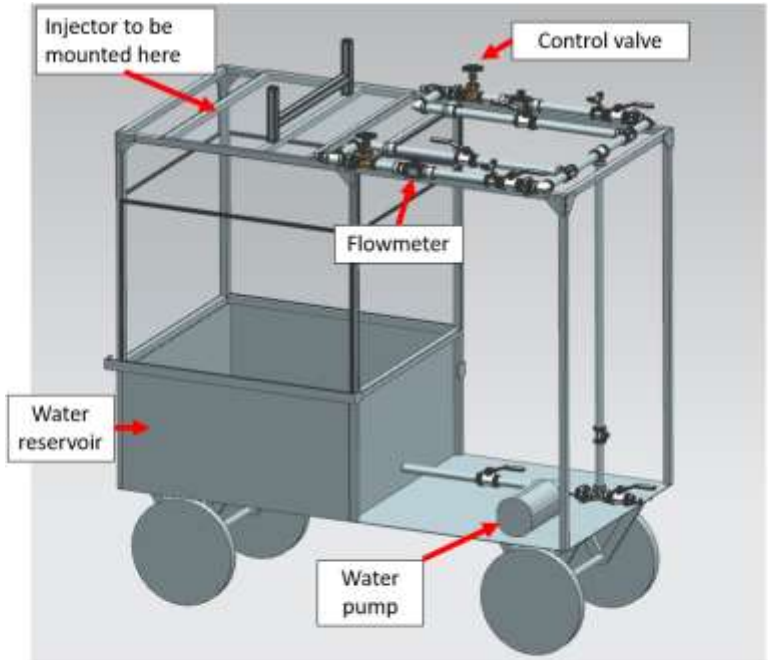

**Figure 41: Water test setup.**

The water test set-up also has the capability to visualize and videotape the water flow as it exits the injector body. This will allow the visualization of the cone half-angle formed by the impingement of the annular and radial flow from the pintle injector. Varying the flow going into one port or the other grants a visualization of the effect the total momentum ratio ($TMR = \frac{(mv)_r}{(mv)_a}$ where: m=mass, v=velocity, r=radial, a=annular [20]) has on the angle of the spray cone. Also, the atomization of the spray will be qualified with the use of a high-speed camera to determine the performance of the pintle injector in this regard.

### 3.2.4 RCE

A calculation was made to approximate the amount of RCEs required to perform the roll maneuver as specified on the flight profile in less than 8 seconds. In order to provide a coupled moment, a minimum of 2 RCE must be fired simultaneously; therefore, to perform the roll

maneuver at least 4 RCE must be mounted on the vehicle structure: 2 for clockwise rotation and 2 for counter-clockwise rotation as shown in Figure 44. However, due to the time restriction to do a whole 360° roll, the possibility of requiring more than a single pair of RCE per burn became apparent.

The geometry of the vehicle was assumed as a solid cuboid with a height of 13 ft. and a width and depth of 3.8 ft. The mass of 1,350 lbm was assumed to be evenly distributed among the whole geometry. An estimation of the time required to perform the 360° roll was made assuming constant firing over the whole maneuver. Using the equation of angular motion with constant acceleration, the time required to perform half a turn (180°) was calculated and then doubled to find the total time required for the complete maneuver: $t = \sqrt{2\theta/_{\alpha}}$ where t=time, θ=final position (180°) α=angular acceleration. Since α is a function of the torque generated by the RCS, increasing the number of RCE firing simultaneously decreases the time required for the roll maneuver.

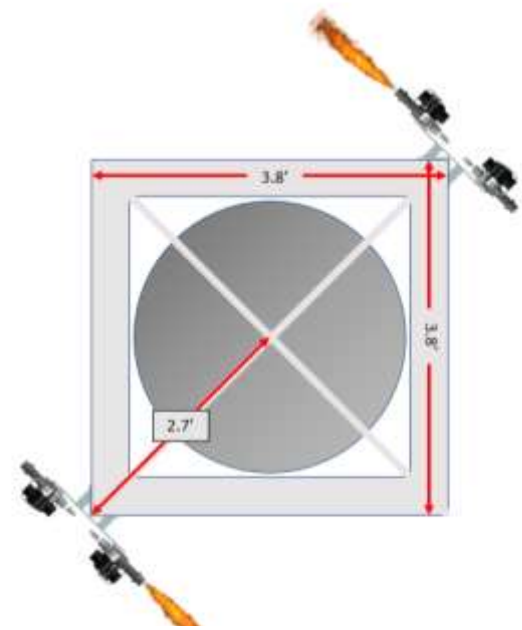

**Figure 42: Top view of RCS mounting configuration.**

It was found that by having the minimum number of RCE (4) required approximately 9.7s to complete the roll maneuver. Given that only 8s had been assigned for this maneuver, the calculation was repeated by adding an extra pair of RCE per side. With a total of 8 RCE the maneuver would require a minimum of 6.9s. However, it might prove more beneficial to extend the allotted maneuver time rather than mounting so many Pencil thrusters.

The Pencil thruster design at the cSETR has seen extensive testing in the past year. Similar to the process that will be done with the CROME-X engine, this RCE was first subjected to a water-flow test. The objective of these tests was to obtain injector pressure drop vs flowrate data using water. By knowing the relation that the flow rate has with pressure drop through the injection,

the behavior of the flowing fluids is better understood and allows the development of the test matrices to be followed during hot-fire tests [15]. The water tests were performed by connecting the RCE to a tank filled with water. The ullage in the water tank was then pressurized to different pressures ranging between 20 and 80 psig in increments of 10 psi resulting in a wide range of flowrates. The flowrate was measured by using a turbine flowmeter while pressure transducers read the static pressure upstream of the engine valves in order to measure the pressure drop. This data could then be related to flow performance using $LO_2$ and $LCH_4$ by adjusting for density. Although the water test results did not match the predicted values for flow and pressure drop (the $C_d$ value was larger than expected) the test data was used to determine the required tank pressures that would result in the desired flow rates during hot-fire tests.

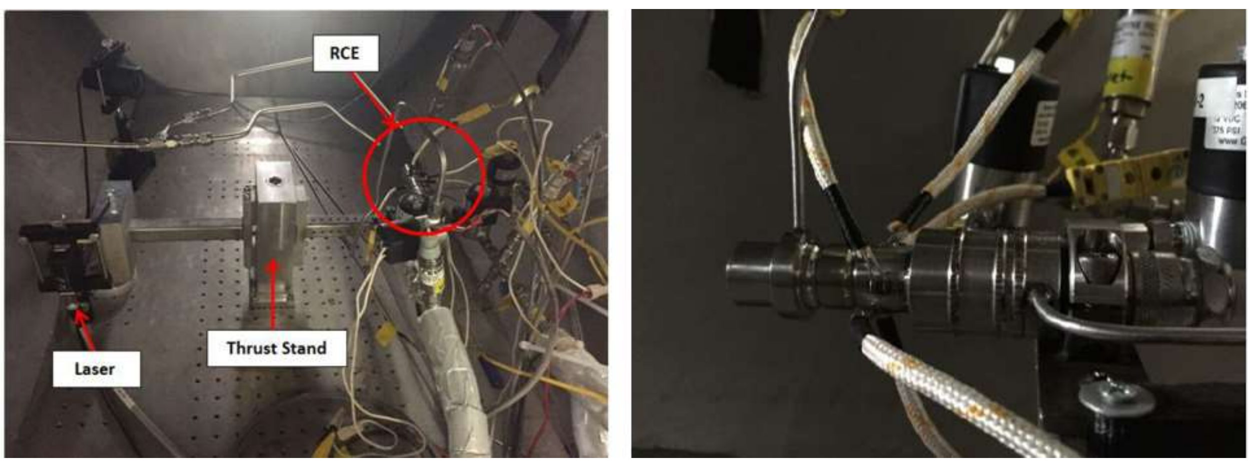


**Figure 43: RCE mounted on TTS [15].**

Once the water tests were completed, preparations for hot-fire tests began. The Pencil thruster was mounted on a torsional thrust stand (TTS) designed in-house. A laser is used to measure the displacement caused on the TTS by the thrust of the vehicle and in order to correlate that displacement to a thrust measurement, the TTS was first calibrated by hanging weights from one end and recording the ensuing deflection from the laser. This allowed a calibration curve to be generated through the thrust range expected by the RCE.

Initially, the hot-fire tests were done with gaseous propellants. Although the RCE was designed for liquid propellant operation, it was desired to understand how it performed under different propellant conditions. A total of three tests were done at different MR with gaseous

propellants. A maximum thrust output of 0.4 lbf was read from the TTS and the chamber pressure did not exceed 19.3 psia which is much lower than the expected 5 lbf of thrust and 100 psia of $P_c$. With these tests, it was concluded that with the current design the operation of the RCS with gaseous propellants would not be ideal. The low performance was attributed to the high pressure drop experienced by the gaseous propellants through the injector; however, the possibility of instrumentation error was not ruled out [15].

Tests with liquid propellants followed after the gas tests had been completed. Tests were done at low MR in order to maintain the combustion temperature as low as possible. It was quickly found, however, that the performance with liquid propellants was very similar to that seen with the gaseous propellants. The maximum thrust measured was of 0.5 lbf and a maximum $P_c$ of 18 psia. Due to these unacceptable results, a failure investigation ensued.

To determine the cause of failure of the RCE, the first approach was to water test the injector again with the purpose of comparing the results with the original water test that was done. After the first few tests, it was evident that the flow was significantly lower at similar $\Delta P$ than the previous water test. Upon inspection with a borescope, large chunks of Teflon tape were found to be stuck on some of the injection orifices. Figure 46 depicts one of the larger pieces of Teflon found.

**Figure 44: Teflon tape stuck inside $LO_2$ orifice [24].**

A cleaning procedure was done which including flowing high pressure $GN_2$ repeatedly. With this method, a large amount of Teflon tape was visibly removed from the RCE. It was then subjected to water test again in order to find if the clogs had been removed. This time, the results resembled the results found in the original water-flow tests on the $LO_2$ side. The $LCH_4$

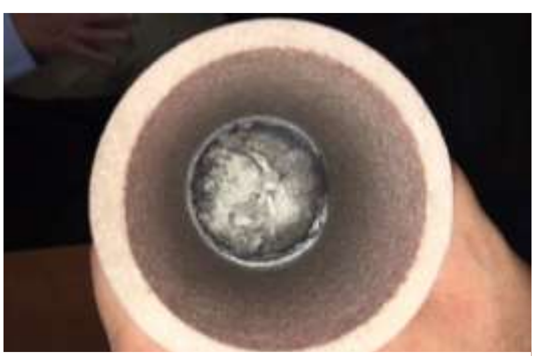

**Figure 45: Melted pencil thruster inside ceramic crucible [21].**

side however, still showed sub-ideal performance and a more aggressive method of cleaning was deemed necessary. With the idea of melting away any remnant of Teflon still in the RCE, it was introduced in a furnace at 1000°C for 24 hours. Unfortunately, during this process, a malfunction occurred to the furnace and it overheated to a temperature of 1800°C completely melting the Pencil thruster which was made out of Inconel 718 [21].

A new RCS is currently in the process of being sent out for manufacturing with a very similar design except for some small modifications. Figure 48 shows the CAD of the Pencil thruster that will be manufactured next. The modification consists of replacing the inlet manifolds, the new design incorporates ¼" compression tube fittings as opposed to the original 1/8" tubes that were welded to the RCE assembly. The new engine is expected to be delivered by the end of June 2017 in order for it to be hot-fire tested in July of the same year [21].

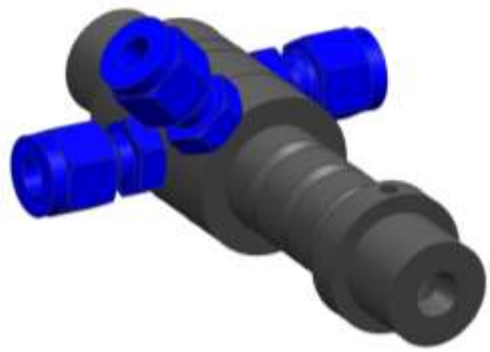

**Figure 46: New RCE assembly [21].**

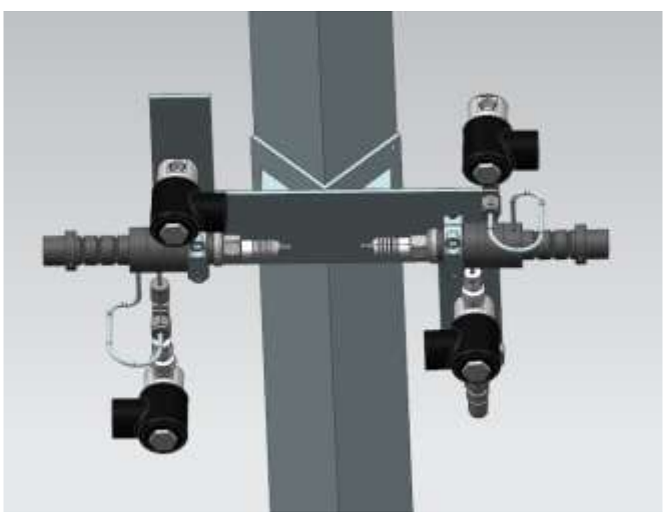

**Figure 47: RCE attached to Janus structure.**

Integration of the RCE to the Janus vehicle will be done by attaching it via a structure as shown in Figure 49. Each RCE module would contain a pair of Pencil thrusters pointing in opposite directions as well as their corresponding valves. The module has been designed to be attached to the corner of the vertical beams of the Janus structure. A minimum of two of these modules is required to be attached in a manner as depicted in Figure 44.

### 3.2.5 Torch Igniter

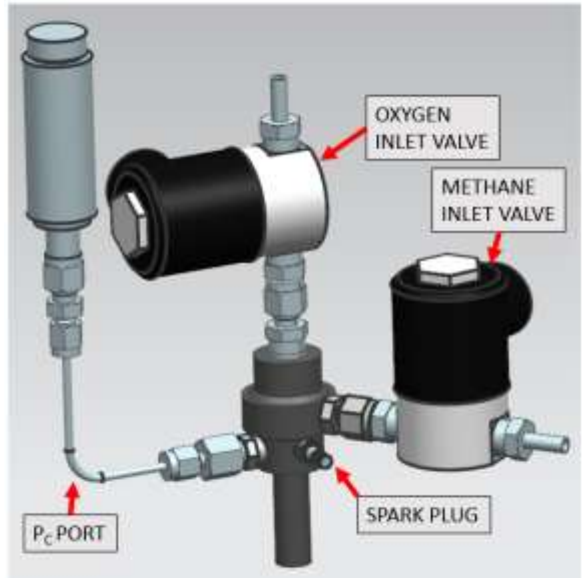


**Figure 48: Torch igniter assembly.**

Several iterations of the Torch igniter have been developed and tested at the cSETR in the past. The last iteration was done with a design as the one shown in Figure 50 which was patented by the cSETR and is ready to be included on both the CROME and CROME-X engine.

The torch igniter was tested under a wide variety of propellant conditions and the level of success of each was measured by the length of the flame produced by it. It was found that when the propellants being injected were at gaseous conditions 100% ignition rate could be achieved. However, as the tests were shifted towards liquid condition propellants, ignition became harder to achieve and many of the tests were unsuccessful.

Initial tests of the CROME-X engine on the J-1a configuration will be done in order to confirm whether the igniter operates reliably under the Janus fluid system configuration. In the case that those tests are not successful, the igniter will be fed gaseous methane and oxygen coming from a separate gas cylinders; however, that would only be done under the J-1a prototype. For the J-1b and subsequent prototypes, a method of storing propellants at the necessary gaseous conditions for the igniter will be incorporated within the CROME-X module. The P&ID depicted in Figure 51 below, describes a possible method for storing gaseous propellants within the main engine feed system. The gas containers labeled E-1 and E-2 would be sample cylinders filled with sufficient $GO_2$ and $LCH_4$ to perform a specific amount of main engine starts. In the case that the igniter operates reliably during the initial tests on the J-1a configuration this will not be necessary and the igniter will be fed from taps coming out of the main propellant lines.

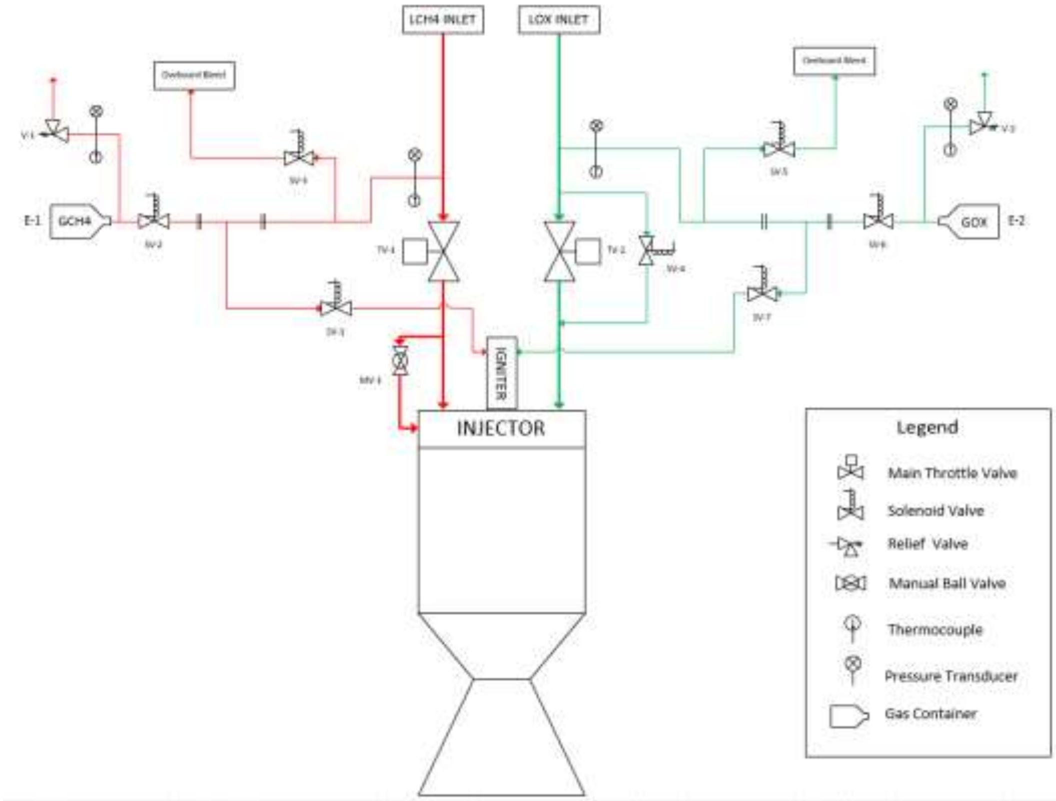


**Figure 49: CROME-X P&ID with stored gaseous propellants for the torch igniter.**

# Chapter 4: Summary and Conclusion

The cSETR has focused on the development of $LO_2$-$LCH_4$ propulsion technologies. Janus is a robotic lander that will be used as a testbed for these propulsion technologies and to demonstrate their integrated operation in a vehicle. The final goal of Janus is to perform a fully autonomous flight on which it ascends to a height of 20’, performs a roll maneuver using RCS, and descends and lands back on the ground.

The development of the vehicle will be done incrementally through prototypes. Each subsequent prototype will incorporate new technologies to eventually have the capability of performing the full mission profile.

Some of these technologies such as the torch igniter and the Pencil RCE have been tested at the Goddard Combustion and Propulsion Research Facility in UTEP. However, larger rocket engines such as the CROME 500 lbf and CROME-X 2,000 lbf engines cannot be tested at that facility and thus require a higher capacity test stand. Therefore, the initial iterations of the Janus vehicle will serve as the test stand for these engines. The cSETR is currently building tRIAc, a new testing facility in Fabens, TX. The high-thrust engine tests will be done there as well as the eventual flights of the Janus vehicle.

A set of requirements has been established for the vehicle as a whole as well as for its subsystems. At the same time, progress has been done individually on the design and testing of most of the subsystems. An initial conceptual design of the integration of the vehicle has also been laid out. The documentation of this work will serve as a tool for the new team members to carry the project forward by explaining the reasoning behind the decisions made and the process taken.

Some of the most immediate future steps are:

- Finalize CROME-X component testing.
- Manufacture CROME-X injector and test it by flowing water.
- Manufacture and hot-fire test new RCE.
- Procurement of propellant test tanks.

- Manufacture and assemble J-1a structures, fluid system and instrumentation.
- Develop test procedures for the CROME-X hot-fire tests.
- Manufacture and assemble the rest of the CROME-X engine.
- Test CROME-X under the J-1a configuration.

# References


[1] J. E. Kleinhenz and A. Paz, "An ISRU Propellant Production System to Fully Fuel a Mars Ascent Vehicle," in *AIAA SciTech Forum*, Gapevine, Texas, 2017.

[2] D. K. Huzel and D. H. Huang, Modern Engineering for Design of Liquid-Propellant Rocket Engines, American Institute of Aeronautics and Astronautics, Inc, 1992.

[3] E. A. Hurlbert, R. Whitley, M. D. Klem, W. Johnson, L. Alexander, E. D'Aversa, J.-M. Ruault, C. Manfletti, J.-N. Caruana, H. Ueno and H. Asakawa, "International Space Exploration Coordination Group Assessment of Technology Gaps for LOx/Methane Systems for the Global Exploration Roadmap," in *AIAA Space 2016*, Long Beach, CA, 2016.

[4] M. D. Klem, T. D. Smith, M. F. Wadel, M. L. Meyer, J. M. Free and H. A. I. Cikanek, "Liquid Oxygen/Liquid Methane Propulsion and Cryogenic Advancement Development," in *62nd International Astronautical Congress*, Cape Town, South Africa, 2011.

[5] J. C. I. Melcher and J. K. Allred, "Liquid Oxygen/Liquid Methane Test Results of the RS-18 Lunar Ascent Engine at Simulated Altitude Conditions at NASA White Sands Test Facility," in *45th AIAA/ASME/SAE/ASEE Joint Propulsion*, Denver, CO, 2009.

[6] J. Collins, E. Hurlbert, K. Romig, J. Melcher, A. Hobson and P. Eaton, "Sea-Level Flight Demonstration and Altitude Characterization of a LO2/LCH4 Based Accent Propulsion Lander," in *45th AIAA/ASME/SAE/ASEE Joint Propulsion Conference and Exhibit*, Denver, CO, 2009.

[7] E. Musk, "Making Humans a Multiplanetary Species Presentation," in *67th International Astronautical Congress*, Guadalajara, Mexico, 2016.

[8] A. G. Belluscio, "ITS Propulsion - The Evolution of the SpaceX Raptor Engine," NASASpaceFlight.com, 3 October 2016. [Online]. Available: https://www.nasaspaceflight.com/2016/10/its-propulsion-evolution-raptor-engine/. [Accessed 16 March 2017].

[9] Blue Origin, "Our Approach to Technology," Blue Origin, n.d.. [Online]. Available: https://www.blueorigin.com/technology. [Accessed 19 March 2017].

[10] J. Hart and J. Devolites, "Morpheus Vertical Test Bed Flight Testing," in *2014 IEEE Aerospace Conference*, Big Sky, MT, 2014.

[11] R. L. Morehead, "Project Morpheus Main Engine Development and Preliminary Flight Testing," in *47th AIAA Joint Propulsion Conference*, San Diego, CA, 2011.

[12] J. C. Melcher and R. L. Morehead, "Combustion Stability Characteristics of the Project Morpheus Liquid Oxygen / Liquid Methane Main Engine," in *50th AIAA/ASME/SAE/ASEE Joint Propulsion Conference* , Cleveland, OH, 2014.

[13] I. Lopez, L. I. Bugarin, R. Ponce and A. Choudhuri, "Janus: LOX/LCH4 Robotic Lander Testbed," in *The Southwest Emerging Technology Symposium*, El Paso, TX, 2016.

[14] G. A. Dressler and J. M. Bauer, "TRW Pintle Engine Heritage and Performance Characteristics," in *36th AIAA/ASME/SAE/ASEE Joint Propulsion Conference and Exhibit*, Huntsville, AL, 2000.

[15] A. Johnson, "Design and Performance Evaluations of a LO2/Methane Reaction Control Engine," The University of Texas at El Paso, El Paso, 2016.

[16] E. A. Hurlbert, J. P. McManamen, J. Sooknanen and J. W. Studak, "Advanced Development of a Compact 5-15 lbf Lox/Methane Thruster for an Integrated Reaction Control and Main Engine Propulsion System," in *47th AIAA/ASME/SAE/ASEE Joint Propulsion Conference*, San Diego, CA, 2011.

[17] A. J. Moreno, M. B. Garcia, M. Chaidez, R. Ponce, J. R. Adams and A. Choudhuri, "Structural Design Concept for a Static Test Bed," in *The Southwest Emerging Technology Symposium*, El Paso, TX, 2017.

[18] Y. A. Çengel and J. M. Cimbala, Fluid Mechanics Fundamentals and Applications, Boston, MA: McGraw Hill Higher Education, 2006.

[19] P. Nunez, L. Hernandez, I. Lopez and A. Choudhuri, "Hardware Development and Testing for a LOX/LCH4 2000 lbf Rocket Engine," in *The Southwest Emerging Technology Symposium*, El Paso, TX, 2017.

[20] I. Lopez, A. Johnson, A. Patel, R. Ponce, M. Lopez, E. Flores, G. Martinez and A. Choudhuri, "Design and Water Flow Testing of a LOX/LCH4 Pintle Injector," in *5th Southwest Energy Science and Engineering Symposium*, El Paso, TX, 2015.

[21] S. Torres, "RCE Failure Report," N.p., El Paso, TX, 2017.

[22] M. Chaidez, "Structural Design of Liquid Oxygen / Liquid Methane Robotic Lander Janus," The University of Texas at El Paso, El Paso, TX, 2016.

[23] C. D. Brown, Spacecraft Propulsion, Washington D.C.: American Institute of Aeronautics and Astronautics, Inc., 1995.

[24] S. Torres, D. Ott, R. Ponce and A. Choudhuri, "Lessons Learned: Reaction Control Engine Failure Investigation," in *Southwest Emerging Technology Symposium*, El Paso, TX, 2017.

# Glossary

| | |
|---|---|
| **ALHAT** | Autonomous Landing and Hazard Avoidance Technology |
| **AME** | Ascent Main Engine |
| **ATK** | Alliant Techsystems |
| **C*** | Characteristic exhaust velocity |
| **CAD** | Computer Aided Design |
| **CEA** | Chemical Equilibrium with Applications |
| **CoM** | Center of Mass |
| **COTS** | Commercial off-the-shelf |
| **CROME** | Centennial Restartable Oxygen Methane Engine |
| **cSETR** | Center for Space Exploration Technology Research |
| $C_v$ | Flow Coefficient |
| **DAQ** | Data Acquisition |
| **DOF** | Degree-of-freedom |
| **ESAS** | Exploration System Architecture Study |
| **FEA/FEM** | Finite Element Analysis / Model |
| **FFC** | Fuel Film Cooling |
| **FS** | Factor of Safety |
| **ft.** | Foot; unit of length |
| **g** | Unit of acceleration corresponding to a multiple of acceleration due to gravity |
| $GN_2$ | Gaseous Nitrogen |
| **GNC** | Guidance Navigation and Control |
| **GRC** | NASA Glenn Research Center |
| **He** | Helium |
| **HHFTF** | High Heat Flux Test Facility |
| **ID** | Inner Diameter |

| | |
|---|---|
| **$I_{sp}$** | Specific impulse |
| **ISRU** | In-situ Resource Utilization |
| **ITS** | SpaceX Interplanetary Transport System |
| **JSC** | NASA Johnson Space Center |
| **KSC** | NASA Kennedy Space Center |
| **KTE** | KT Engineering |
| **lbf** | Pound-force; unit of force |
| **lbm** | Pound-mass; unit of mass |
| **$LCH_4$** | Liquid Methane |
| **LCM** | Load Cell Module |
| **$LH_2$** | Liquid Hydrogen |
| **LM** | Apollo Lunar Module |
| **$LN_2$** | Liquid Nitrogen |
| **LNG** | Liquefied Natural Gas |
| **$LO_2$** | Liquid Oxygen |
| **LSAM** | Lunar Surface Access Module |
| **MDC** | Mission Duty Cycle |
| **MIRO** | MUREP Institutional Research Opportunity |
| **MR** | Propellant Mixture Ratio (also O/F) |
| **MUREP** | Minority University Research and Education Project |
| **$N_2O_4$** | Dinitrogen Tetroxide |
| **NASA** | National Aeronautics and Space Administration |
| **OD** | Outer Diameter |
| **O/F** | Oxidizer to fuel mixture ratio (also MR) |
| **P&ID** | Piping and Instrumentation Diagram |
| **$P_c$** | Combustion chamber pressure |
| **PL** | Power Level (as a percentage of a rocket engine's maximum thrust capability) |

| | |
|---|---|
| **psig/psia** | Pounds per square inch gauge / pounds per square inch absolute |
| **PT** | Pressure Transducer |
| **RCS/RCE** | Reaction Control System/Engine |
| **RP-1** | Rocket Propellant 1 (highly refined kerosene) |
| **RPM** | Revolutions Per Minute |
| **SOFC** | Solid Oxide Fuel Cell |
| **SSC** | NASA Stennis Space Center |
| **SSME** | Space Shuttle Main Engine |
| **TC** | Thermocouple |
| **TMR** | Total Momentum Ratio |
| **tRIAc** | Technology Research and Innovation Acceleration Park |
| **TTS** | Torsional Thrust Stand |
| **ULA** | United Launch Alliance |
| **UTEP** | The University of Texas at El Paso |
| **V-A** | Valve – Actuator Connector |
| **VTOL** | Vertical take-off and landing |
| **WSTF** | NASA White Sands Test Facility |

# Vita

Raul Ponce was born in El Paso, Texas and raised in Parral, Mexico. After completing high school, he returned to El Paso where he attended the University of Texas at El Paso (UTEP) and obtained a Bachelor's of Science degree in Mechanical Engineering in May, 2015. During his undergraduate degree, he began working at the Center for Space Exploration Technology Research (cSETR) as an undergraduate research assistant. Upon graduation, he decided to continue his education and pursue a Master's of Science degree at UTEP while continuing his research at the cSETR.

Raul served for three internships at the National Aeronautics and Space Administration (NASA). His first internship was under the Engineering and Test Directorate of Stennis Space Center (SSC) in Mississippi during the summer of 2015. His second and third internships were as a Pathways Intern under the Structural Mechanics Branch of Glenn Research Center (GRC) in Cleveland, Ohio in the fall and summer of 2016.

Raul has accepted a job offer with Lockheed Martin Space Systems Company as a Systems Engineer Associate in Sunnyvale, California. He will begin working there after receiving his Master's of Science in Mechanical Engineering.

Contact Information: rponce4@miners.utep.edu or ponce_raul@ymail.com

This thesis was typed by Raul Ponce.